1

Ocular Embryology and Congenital Malformations

Cynthia S. Cook

Veterinary Vision, San Carlos and San Francisco, CA, USA

An understanding of normal and abnormal ocular development is essential to the broader subjects of anatomy, physiology, and pathology. Embryology provides both insight into the development of structures such as the cornea, iridocorneal angle, and retina and their normal and pathologic functions, as well as a means of understanding how congenital malformations occur.

Investigations of ocular development have often used rodents as animal models. Comparison with studies of humans and other animals demonstrates that the sequence of developmental events is very similar across species (Cook, 1995; Cook & Sulik, 1986; Hilfer, 1983; O'Rahilly, 1983). Factors that must be considered when making interspecies comparisons include duration of gestation, differences in anatomic end point (e.g., presence of a tapetum, macula, or Schlemm's canal), and when eyelid fusion breaks (during the sixth month of gestation in the human versus 2 weeks postnatal in the dog; Table 1.1).

This chapter describes normal events and abnormalities in this developmental sequence that can lead to malformations. Bearing in mind the species differences alluded to earlier, the mouse is a valuable model in the study of normal and abnormal ocular morphogenesis. In particular, studying the effects of acute exposure to teratogens during development has provided valuable information about the specific timing of events that lead to malformations.

Gastrulation and Neurulation

Cellular mitosis following fertilization results in transformation of the single-cell zygote into a cluster of 12–16 cells. With continued cellular proliferation, this morula becomes a blastocyst, containing a fluid-filled cavity. The cells of the blastocyst will form both the embryo proper and the extraembryonic tissues (i.e., amnion and chorion). At this early stage, the embryo is a bilaminar disc, consisting of hypoblast and epiblast. This embryonic tissue divides the blastocyst space into the amniotic cavity (adjacent to epiblast) and the yolk sac (adjacent to hypoblast; Fig. 1.1).

Gastrulation (formation of the mesodermal germ layer) begins during day 10 of gestation in the dog (day 7 in the mouse; days 15–20 in the human). The primitive streak forms as a longitudinal groove within the epiblast (i.e., future ectoderm). Epiblast cells migrate toward the primitive streak, where they invaginate to form the mesoderm. This forms the three classic germ layers: ectoderm, mesoderm, and endoderm. Gastrulation proceeds in a cranial-to-caudal progression; simultaneously, the cranial surface ectoderm proliferates, forming bilateral elevations called the neural folds (i.e., the future brain). The columnar surface ectoderm in this area now becomes known as the neural ectoderm (Fig. 1.2).

As the neural folds elevate and approach each other, a specialized population of mesenchymal cells, the neural crest, emigrates from the neural ectoderm at its junction with the surface ectoderm (Fig. 1.3). Migration and differentiation of the neural crest cells are influenced by the hyaluronic acid-rich extracellular matrix. This acellular matrix is secreted by the surface epithelium as well as by the crest cells, and it forms a space through which the crest cells migrate. Fibronectin secreted by the noncrest cells forms the limits of this mesenchymal migration (LeDouarin & Teillet, 1974). Interactions between the migrating neural crest and the associated mesoderm appear to be essential for normal crest differentiation (LeDouarin & Teillet, 1974; Noden, 1993). The neural crest cells migrate peripherally beneath the surface ectoderm to spread throughout the embryo, populating the region around the optic vesicle and ultimately giving rise to nearly all the connective tissue structures of the eye (Table 1.2; Hilfer & Randolph, 1993; Johnston et al., 1979; Noden, 1993). The patterns of neural crest emergence and migration correlate with the segmental disposition of the developing brain.

Veterinary Ophthalmology: Volume I, Sixth Edition. Edited by Kirk N. Gelatt, Gil Ben-Shlomo, Brian C. Gilger, Diane V.H. Hendrix, Thomas J. Kern, and Caryn E. Plummer.
© 2021 John Wiley & Sons, Inc. Published 2021 by John Wiley & Sons, Inc.
Companion website: www.wiley.com/go/gelatt/veterinary

Table 1.1 Sequence of ocular development (Cook, 1995; O'Rahilly, 1983).

Human (Approximate Postfertilization Age)				Dog (Day Postfertilization)	
Month	**Week**	**Day**	**Mouse (Day Postfertilization)**	**Postnatal (P)**	**Developmental Events**
1	3	22	8	13	Optic sulci present in forebrain
	4	24	9	15	Optic sulci convert into optic vesicles
			10	17	Optic vesicle contacts surface ectoderm
					Lens placode begins to thicken
		26			Optic vesicle surrounded by neural crest mesenchyme
2	5	28	10.5		Optic vesicle begins to invaginate, forming optic cup
					Lens pit forms as lens placode invaginates
					Retinal primordium thickens, marginal zone present
		32	11	19	Optic vesicle invaginated to form optic cup
					Optic fissure delineated
					Retinal primordium consists of external limiting membrane, proliferative zone, primitive zone, marginal zone, and internal limiting membrane
					Oculomotor nerve present
		33	11.5	25	Pigment in outer layer of optic cup
					Hyaloid artery enters through the optic cup
					Lens vesicle separated from surface ectoderm
					Retina: inner marginal and outer nuclear zones
			11.5	29	Basement membrane of surface ectoderm intact
					Primary lens fibers form
					Trochlear and abducens nerves appear
					Lid folds present
	6	37	12		Edges of optic fissure in contact
			12	30	Tunica vasculosa lentis present
					Lens vesicle cavity obliterated
					Ciliary ganglion present
		41	12	32	Posterior retina consists of nerve fiber layer, inner neuroblastic layer, transient fiber layer of Chievitz, proliferative zone, outer neuroblastic layer, and external limiting membrane
			17	32	Eyelids fuse (dog)
	7				Anterior chamber beginning to form
			12.5	40	Secondary lens fibers present
		48	14	32	Corneal endothelium differentiated
	8	51			Optic nerve fibers reach the brain
					Optic stalk cavity is obliterated
					Lens sutures appear
					Acellular corneal stroma present
		54		30–35	Scleral condensation present
	9	57	17	40	First indication of ciliary processes and iris
					Extraocular muscles visible

Table 1.1 (Continued)

Human (Approximate Postfertilization Age)			Mouse (Day Postfertilization)	Dog (Day Postfertilization)	
Month	**Week**	**Day**		**Postnatal (P)**	**Developmental Events**
				—	Eyelids fuse (occurs earlier in the dog)
	10			45	Pigment visible in iris stroma
					Ciliary processes touch lens equator
					Rudimentary rods and cones appear
				45–1 P	Hyaloid artery begins to atrophy to the disc
3	12			—	Branches of the central retinal artery form
4				51	Pupillary sphincter differentiates
					Retinal vessels present
				56	Ciliary muscle appears
				—	Eye axis forward (human)
—				56	Tapetum present (dog)
				2–14 P	Tunica vasculosa lentis atrophies
					Short eyelashes appear
5				40	Layers of the choroid are complete with pigmentation
6				—	Eyelids begin to open, light perception
				1 P	Pupillary dilator muscle present
7				1–14 P	Pupillary membrane atrophies
				1–16 P	Rod and cone inner and outer segments present in posterior retina
				10–13 P	Pars plana distinct
9				16–40 P	Retinal layers developed
				14 P	Regression of pupillary membrane, tunica vasculosa lentis, and hyaloid artery nearly complete
					Lacrimal duct canalized

Data from Aguirre et al. (1972), Akiya et al. (1986), Cook (1995), and van der Linde-Sipman et al. (2003).

It is important to note that mesenchyme is a general term for any embryonic connective tissue. Mesenchymal cells generally appear stellate and are actively migrating populations surrounded by extensive extracellular space. In contrast, the term *mesoderm* refers specifically to the middle embryonic germ layer. In other parts of the body (e.g., the axial skeletal system), mesenchyme develops primarily from mesoderm, with a lesser contribution from the neural crest. In the craniofacial region, however, mesoderm plays a relatively small role in the development of connective tissue structures. In the eye, mesoderm probably gives rise only to the striated myocytes of the extraocular muscles and vascular endothelium. Most of the craniofacial mesenchymal tissue comes from neural crest cells (Johnston et al., 1979).

The neural tube closes initially in the craniocervical region with closure proceeding cranially and caudally. Once closure is complete, the exterior of the embryo is fully covered by surface ectoderm, and the neural tube is lined by neural ectoderm. Neural segmentation then occurs to form the specific parts of the brain: forebrain (i.e., prosencephalon), midbrain (i.e., mesencephalon), and hindbrain (i.e., rhombencephalon; see Fig. 1.3 and Fig. 1.4). The optic vesicles develop from neural ectoderm within the forebrain, with the ocular connective tissue derivatives originating from the midbrain neural crest.

Formation of the Optic Vesicle and Optic Cup

The optic sulci are visible as paired evaginations of the forebrain neural ectoderm on day 13 of gestation in the dog (see Fig. 1.3, Fig. 1.4, Fig. 1.5, Fig. 1.6, and Fig. 1.7). The transformation from optic sulcus to optic vesicle occurs

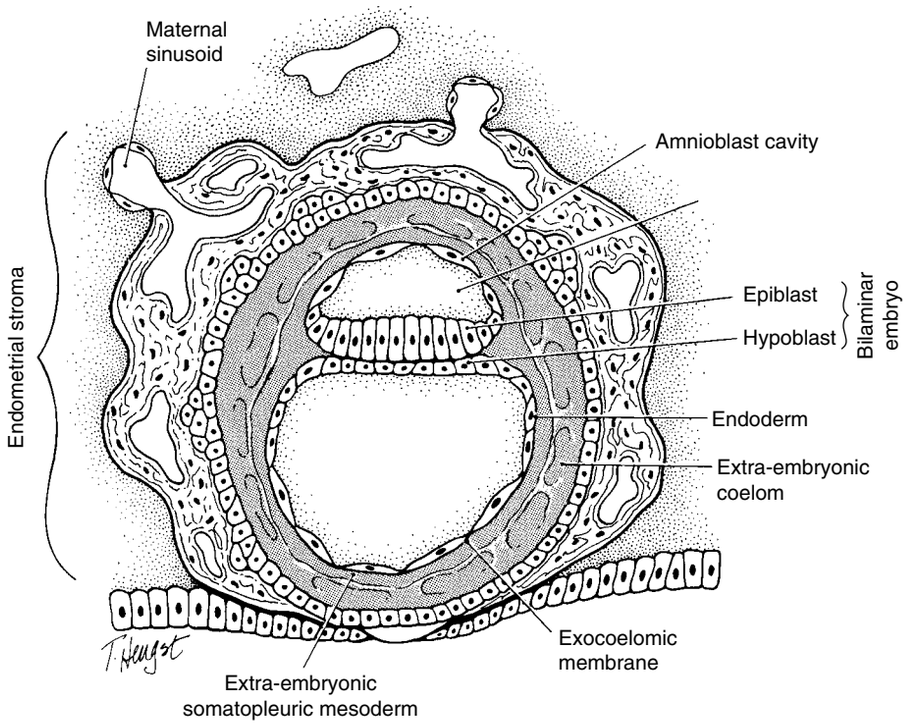

Figure 1.1 A blastocyst that has penetrated the maternal endometrium. An embryoblast has formed and consists of two cell layers: the epiblast above, and the hypoblast below. (Reprinted with permission from Cook, C., Sulik, K.K., & Wright, K.W. (2003) Embryology. In: *Pediatric Ophthalmology and Strabismus* (eds. Wright, K.W. & Spiegel, P.H.), pp. 3–38. New York: Springer.)

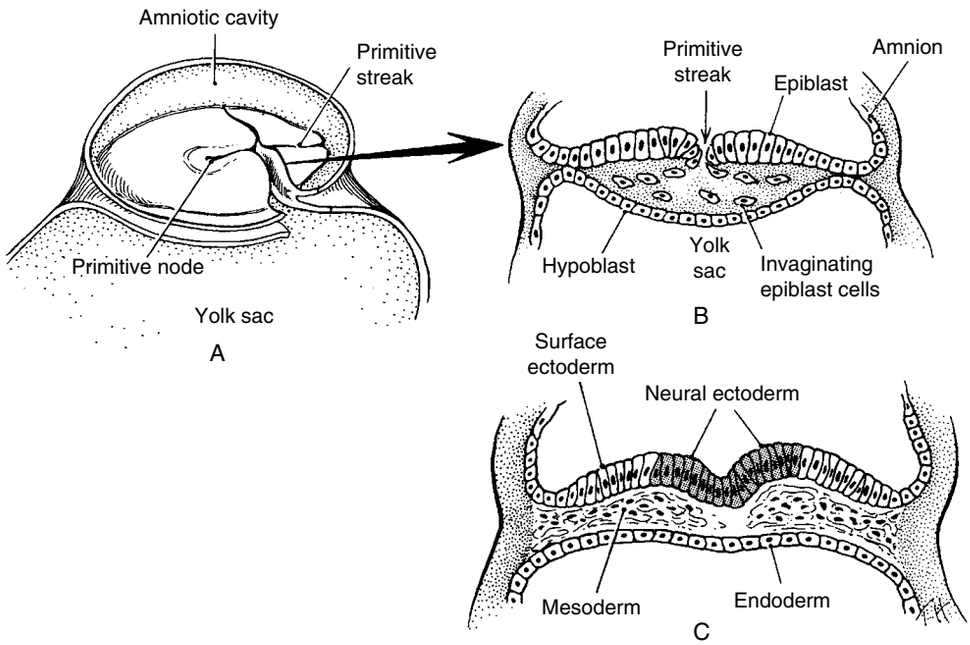

Figure 1.2 **A.** Dorsal view of an embryo in the gastrulation stage with the amnion removed. **B.** Cross-section through the primitive streak, representing invagination of epiblast cells between the epiblast and hypoblast layers. Note that the epiblast cells filling the middle area form the mesodermal layer. **C.** Cross-section through the neural plate. Note that the ectoderm in the area of the neural groove (shaded cells) has differentiated into neural ectoderm, whereas the ectoderm on each side of the neural groove is surface ectoderm (clear water cells). (Reprinted with permission from Cook, C., Sulik, K.K., & Wright, K.W. (2003) Embryology. In: *Pediatric Ophthalmology and Strabismus* (eds. Wright, K.W. & Spiegel, P.H.), pp. 3–38. New York: Springer.)

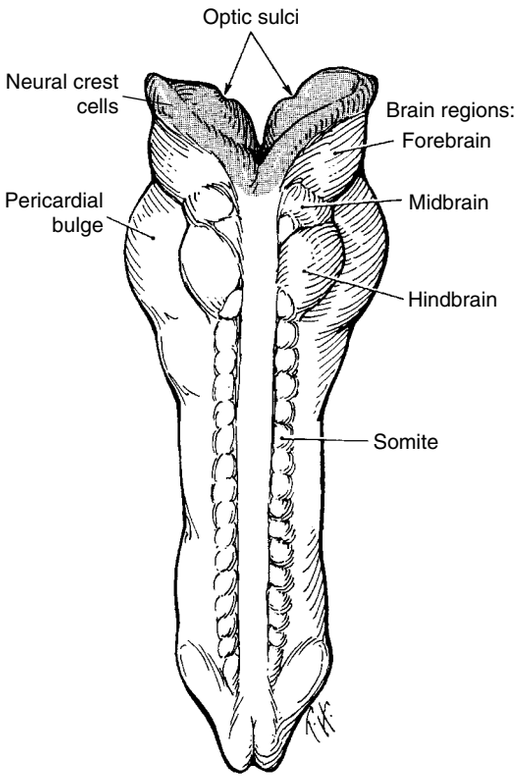

Figure 1.3 Dorsal view showing partial fusion of the neural folds to form the neural tube. Brain vesicles have divided into three regions: forebrain, midbrain, and hindbrain. The neural tube, groove, and facing surfaces of the large neural folds are lined with neural ectoderm (shaded cells), whereas surface ectoderm covers the rest of the embryo. Neural crest cells are found at the junction of the neural ectoderm and surface ectoderm. Neural crest cells migrate beneath the surface ectoderm, spreading throughout the embryo and specifically to the area of the optic sulci. Somites have formed along the lateral aspect of the closed cephalic neural tube. On the inside of both forebrain vesicles is the optic sulci. (Reprinted with permission from Cook, C., Sulik, K.K., & Wright, K.W. (2003) Embryology. In: *Pediatric Ophthalmology and Strabismus* (eds. Wright, K.W. & Spiegel, P.H.), pp. 3–38. New York: Springer.)

concurrent with the closure of the neural tube (day 15 in the dog). Intracellular filaments and microtubules within the cytoskeleton alter cell shape and allow for cell movement. In addition to the mechanical influences of the cytoskeleton and the extracellular matrix, localized proliferation and cell growth contribute to expansion of the optic vesicle (Fig. 1.5; Hilfer & Randolph, 1993; Hilfer et al., 1981).

The optic vesicle enlarges and, covered by its own basal lamina, approaches the basal lamina underlying the surface ectoderm (Fig. 1.5). The optic vesicle appears to play a significant role in the induction and size determination of the palpebral fissure and of the orbital and periocular structures (Jones et al., 1980). An external bulge indicating the presence of the enlarging optic vesicle can be seen at approximately day 17 in the dog.

Table 1.2 Embryonic origins of ocular tissues (Johnston et al., 1979; Noden, 1993; Yamashita & Sohal, 1987).

Neural Ectoderm	Neural Crest
Neural retina	Stroma of iris, ciliary body, choroid, and sclera
Retinal pigment epithelium	Ciliary muscles
Posterior iris epithelium	Corneal stroma and endothelium
Pupillary sphincter and dilator muscle (except in avian species)	Perivascular connective tissue and smooth muscle cells
	Striated muscles of iris (avian species only)
Bilayered ciliary epithelium	Meninges of optic nerve
	Orbital cartilage and bone
	Connective tissue of the extrinsic ocular muscles
	Endothelium of trabecular meshwork
Surface Ectoderm	**Mesoderm**
Lens	Extraocular myoblasts
Corneal and conjunctival epithelium	Vascular endothelium
Lacrimal gland	Schlemm's canal (human)
	Posterior sclera (?)

Data from Ashton (1966), Cook et al. (1991a), and Cook and Sulik (1986, 1988).

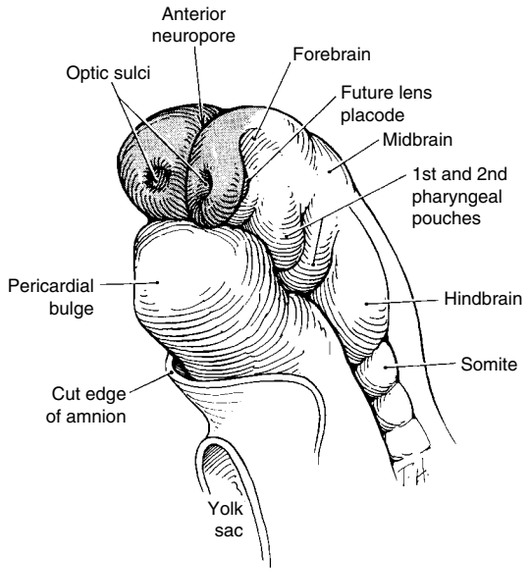

Figure 1.4 Development of the optic sulci, which are the first sign of eye development. Optic sulci on the inside of the forebrain vesicles consisting of neural ectoderm (shaded cells). The optic sulci evaginate toward the surface ectoderm as the forebrain vesicles simultaneously rotate inward to fuse. (Reprinted with permission from Cook, C., Sulik, K.K., & Wright, K.W. (2003) Embryology. In: *Pediatric Ophthalmology and Strabismus* (eds. Wright, K.W. & Spiegel, P.H.), pp. 3–38. New York: Springer.)

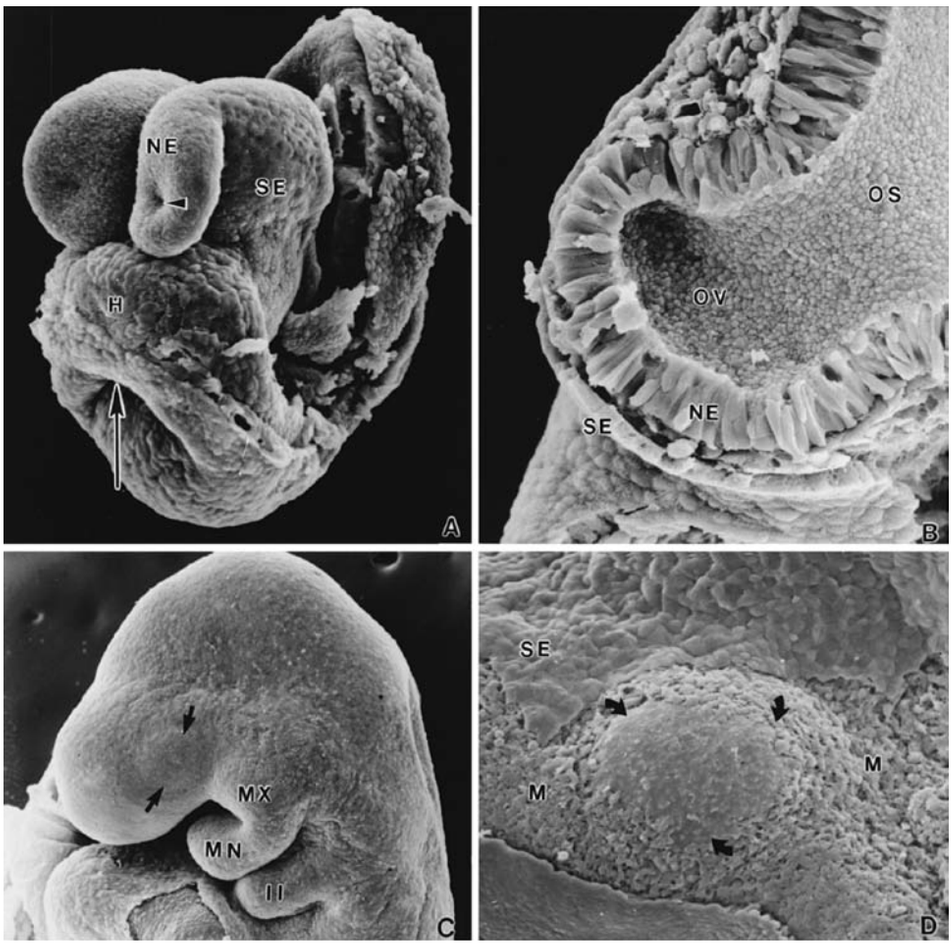

Figure 1.5 **A.** Scanning electron micrograph of a mouse embryo (six somite pairs) on day 8 of gestation, equivalent to day 13 of canine gestation. The amnion has been removed, and the neural folds have segmented into a forebrain region containing the optic sulci (arrowhead), which are evaginations of neural ectoderm (NE). The close proximity to the developing heart (H) can be seen. The area where the NE meets the surface ectoderm (SE) is where the neural fold will meet and fuse; this area also gives rise to the neural crest cells. The entrance to the foregut is indicated by the arrow. **B.** Scanning electron micrograph of the optic vesicle on day 9 of gestation in the mouse (day 15 in the dog). Expansion of the optic sulcus results in an optic vesicle (OV) that approaches the surface ectoderm (SE). A thin layer of mesenchyme is still present between the NE and the SE. The optic stalk (OS) is continuous with the ventricle of the forebrain. **C.** The bulge of the enlarging OV (arrows) can be seen externally. MN, mandibular prominence of the first visceral arch; MX, maxillary prominence of the first visceral arch; II, second visceral arch. **D.** Partial removal of the SE from an embryo of 25 somite pairs (day 17 in the dog; day 19 in the mouse) reveals the exposed basal lamina of the OV (arrows). Enlargement of the optic vesicle has displaced the adjacent mesenchyme (M) so that the basal lamina of the SE is in direct contact with that of the OV. (Reprinted with permission from Cook, C.S. & Sulik, K.K. (1986) Sequential scanning electron microscopic analyses of normal and spontaneously occurring abnormal ocular development in C57B1/6J mice. *Scanning Electron Microscopy*, **3**, 1215–1227.)

The optic vesicle and optic stalk invaginate through differential growth and infolding (Fig. 1.6 and Fig. 1.7). Local apical contraction (Wrenn & Wessells, 1969) and physiologic cell death (Schook, 1978) have been identified during invagination. The surface ectoderm in contact with the optic vesicle thickens to form the lens placode (Fig. 1.6, Fig. 1.7, and Fig. 1.8A, B), which then invaginates with the underlying neural ectoderm. The invaginating neural ectoderm folds onto itself as the space within the optic vesicle collapses, thus creating a double layer of neural ectoderm, the optic cup.

This process of optic vesicle/lens placode invagination progresses from inferior to superior, so the sides of the optic cup and stalk meet inferiorly in an area called the optic (choroid) fissure (Fig. 1.8F). Mesenchymal tissue (of primarily neural crest origin) surrounds and fills the optic cup, and by day 25 in the dog, the hyaloid artery develops from mesenchyme in the optic fissure. This artery courses from the optic stalk (i.e., the region of the future optic nerve) to the developing lens (Fig. 1.9 and Fig. 1.10). The two edges of the optic fissure meet and initially fuse anterior to the optic stalk, with fusion then progressing anteriorly and posteriorly.

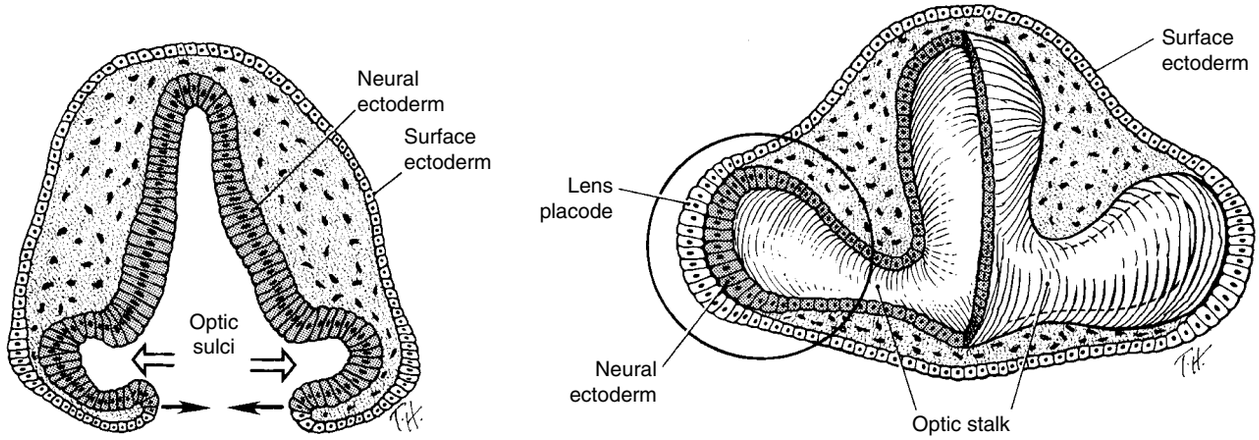

Figure 1.6 Cross-section at the level of the optic vesicle. Note that the neural tube is closed. The surface ectoderm now covers the surface of the forebrain, and the neural ectoderm is completely internalized. The surface ectoderm cells overlying the optic vesicles enlarge to form the early lens placode. (Reprinted with permission from Cook, C., Sulik, K.K., & Wright, K.W. (2003) Embryology. In: *Pediatric Ophthalmology and Strabismus* (eds. Wright, K.W. & Spiegel, P.H.), pp. 3–38. New York: Springer.)

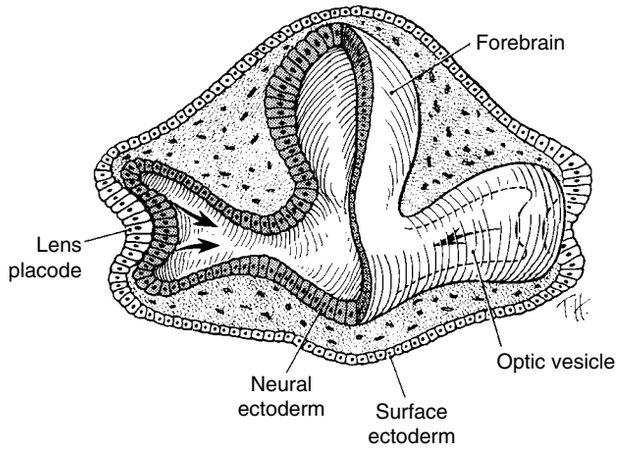

Figure 1.7 Transection showing invaginating lens placode and optic vesicle (arrows), thus creating the lens vesicle within the optic cup. Note the orientation of the eyes 180° from each other. (Reprinted with permission from Cook, C., Sulik, K.K., & Wright, K.W. (2003) Embryology. In: *Pediatric Ophthalmology and Strabismus* (eds. Wright, K.W. & Spiegel, P.H.), pp. 3–38. New York: Springer.)

This process is mediated by glycosaminoglycan-induced adhesion between the two edges of the fissure (Ikeda et al., 1995). Apoptosis has been identified in the inferior optic cup prior to formation of the optic fissure and, transiently, associated with its closure (Ozeki et al., 2000). Failure of this fissure to close normally may result in inferiorly located defects (i.e., colobomas) in the iris, choroid, or optic nerve. Colobomas other than those in the "typical" six o'clock location may occur through a different mechanism and are discussed later.

Closure of the optic cup through fusion of the optic fissure allows intraocular pressure (IOP) to be established. The protein in the embryonic vitreous humor (13% of plasma protein) is derived from plasma proteins entering the eye by diffusion out of permeable vessels in the anterior segment. After day 15, protein content in the vitreous decreases, possibly through dilution with aqueous humor produced by developing ciliary epithelium (Beebe et al., 1986).

Lens Formation

Before contact with the optic vesicle, the surface ectoderm first becomes competent to respond to lens inducers. Inductive signals from the anterior neural plate give this area of ectoderm a "lens-forming bias." Signals from the optic vesicle are required for complete lens differentiation, and inhibitory signals from the cranial neural crest may suppress any residual lens-forming bias in head ectoderm adjacent to the lens (Grainger et al., 1988, 1992). Adhesion between the optic vesicle and surface ectoderm exists, but there is no direct cell contact (Cohen, 1961; Hunt, 1961; Weiss & Jackson, 1961). The basement membranes of the optic vesicle and the surface ectoderm remain separate and intact throughout the contact period.

Thickening of the lens placode can be seen on day 17 in the dog. A tight, extracellular matrix-mediated adhesion between the optic vesicle and the surface ectoderm has been described (Aso et al., 1995; Cook & Sulik, 1988; Garcia-Porrero et al., 1979). This anchoring effect on the mitotically active ectoderm results in cell crowding and elongation and in formation of a thickened placode. This adhesion between the optic vesicle and lens placode also assures alignment of the lens and retina in the visual axis (Beebe, 1985). Abnormal orientation of the optic vesicle as it approaches the surface ectoderm may result in induction of a smaller lens vesicle,

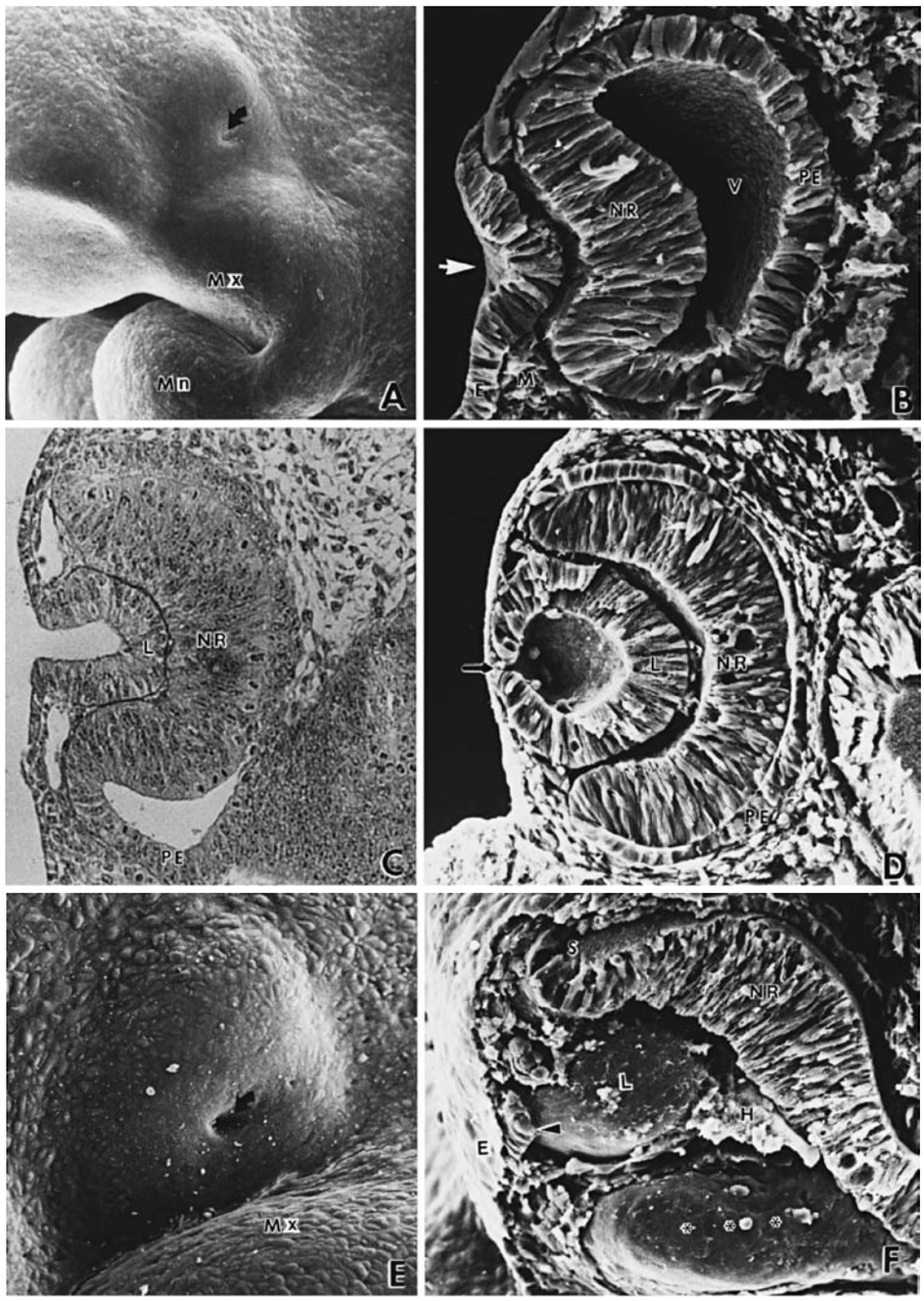

Figure 1.8 **A.** Mouse embryo on day 10 of gestation (29 somite pairs, equivalent to day 17 in the dog). On external examination, the invaginating lens placode can be seen (arrow). Note its position relative to the maxillary prominence (Mx) and mandibular (Mn) prominence of the first visceral arch. **B.** Frontal fracture through the lens placode (arrow) illustrates the associated thickening of the surface ectoderm (E). Mesenchyme (M) of neural crest origin is adjacent to the lens placode. As the precursor to the neural retina (NR), the distal portion of the optic vesicle concurrently thickens, whereas the proximal optic vesicle becomes a shorter, cuboidal layer that is the anlage of the retinal pigment epithelium (PE). The cavity of the optic vesicle (V) becomes progressively smaller. **C.** Light micrograph of the epithelium of the invagination lens placode (L). There is an abrupt transition between the thicker epithelium of the placode and the adjacent surface ectoderm, which is not unlike the transition between the future NR and PE. **D.** As the lens vesicle enlarges, the external opening of lens pore (arrow) becomes progressively smaller. The lens epithelial cells at the posterior pole of the lens elongate to form the primary lens fibers (L). NR, anlage of the neural retina; PE, anlage of the pigment epithelium (now a short cuboidal layer). **E.** External view of the lens pore (arrow) and its relationship to the Mx. **F.** Frontal fracture reveals the optic fissure (*) where the two sides of the invaginating optic cup meet. This forms an opening in the cup, allowing access to the hyaloid artery (H), which ramifies around the invaginating lens vesicle (L). The former cavity of the optic vesicle is obliterated except in the marginal sinus (S), at the transition between the NR and the PE. E, surface ectoderm. (Panels **B** and **F** reprinted with permission from Cook, C.S. & Sulik, K.K. (1986) Sequential scanning electron microscopic analyses of normal and spontaneously occurring abnormal ocular development in C57B1/6J mice. *Scanning Electron Microscopy,* **3**, 1215–1227; panels **C**, **D**, and **E** reprinted with permission from Cook, C. (1995) Embryogenesis of congenital eye malformations. *Veterinary and Comparative Ophthalmology*, **5**, 109–123.)

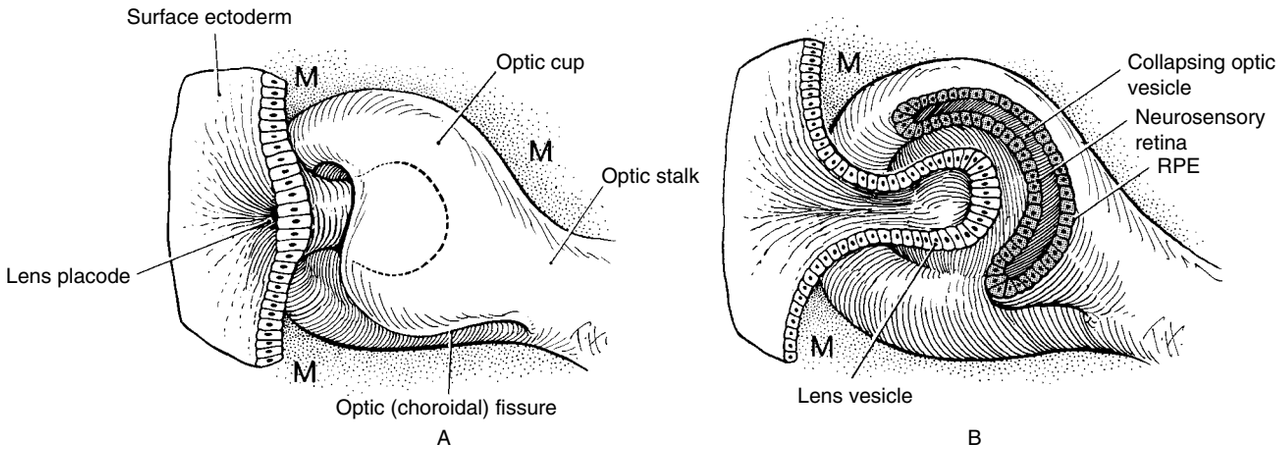

Figure 1.9 Formation of the lens vesicle and optic cup. Note that the optic fissure is present, because the optic cup is not yet fused inferiorly. **A.** Formation of lens vesicle and optic cup with inferior choroidal or optic fissure. Mesenchyme (M) surrounds the invaginating lens vesicle. **B.** Surface ectoderm forms the lens vesicle with a hollow interior. Note that the optic cup and optic stalk are of surface ectoderm origin. (Reprinted with permission from Cook, C., Sulik, K.K., & Wright, K.W. (2003) Embryology. In: *Pediatric Ophthalmology and Strabismus* (eds. Wright, K.W. & Spiegel, P.H.), pp. 3–38. New York: Springer.)

Figure 1.10 Cross-section through optic cup and optic fissure. The lens vesicle is separated from the surface ectoderm. Mesenchyme (M) surrounds the developing lens vesicle, and the hyaloid artery is seen within the optic fissure. (Reprinted with permission from Cook, C., Sulik, K.K., & Wright, K.W. (2003) Embryology. In: *Pediatric Ophthalmology and Strabismus* (eds. Wright, K.W. & Spiegel, P.H.), pp. 3–38. New York: Springer.)

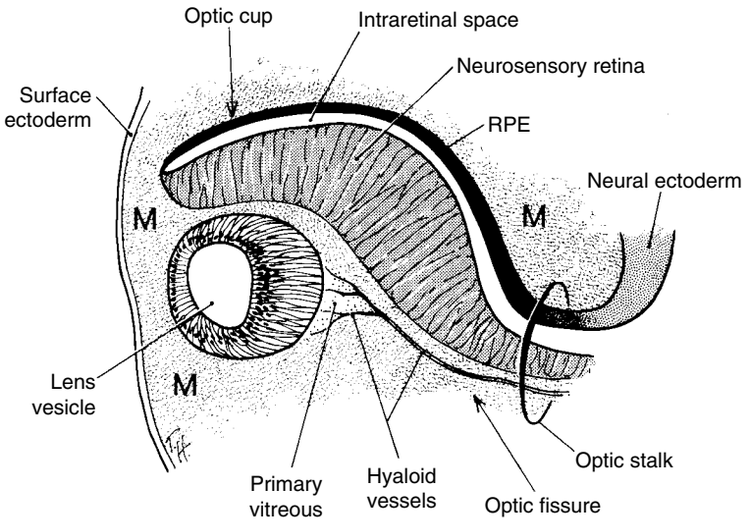

which may assume an abnormal location within the optic cup (Cook & Sulik, 1988).

The lens placode invaginates, forming a hollow sphere, now referred to as a lens vesicle (Fig. 1.8C, D, Fig. 1.9, and Fig. 1.10). The size of the lens vesicle is determined by the contact area of the optic vesicle with the surface ectoderm and by the ability of the latter tissue to respond to induction. Aplasia may result from failure of lens induction or through later involutions of the lens vesicle, either before or after separation from the surface ectoderm (Aso et al., 1995).

Lens vesicle detachment is the initial event leading to formation of the chambers of the ocular anterior segment. This process is accompanied by active migration of epithelial cells out of the keratolenticular stalk, cellular necrosis, apoptosis, and basement membrane breakdown (Garcia-Porrero et al., 1979; Ozeki et al., 2001). Induction of a small lens vesicle that fails to undergo normal separation from the surface ectoderm is one of the characteristics of the teratogen-induced anterior segment dysgenesis described in animal models (Cook & Sulik, 1988). Anterior lenticonus and anterior capsular cataracts as well as anterior segment dysgenesis may result from faulty keratolenticular separation. Additional discussion of anterior segment dysgenesis occurs later in this chapter.

Following detachment from the surface ectoderm (day 25 in the dog), the lens vesicle is lined by a monolayer of cuboidal cells surrounded by a basal lamina, the future lens capsule. The primitive retina promotes primary lens fiber formation in the adjacent lens epithelial cells. Surgical rotation of the chick lens vesicle by 180° results in elongation of the lens epithelial

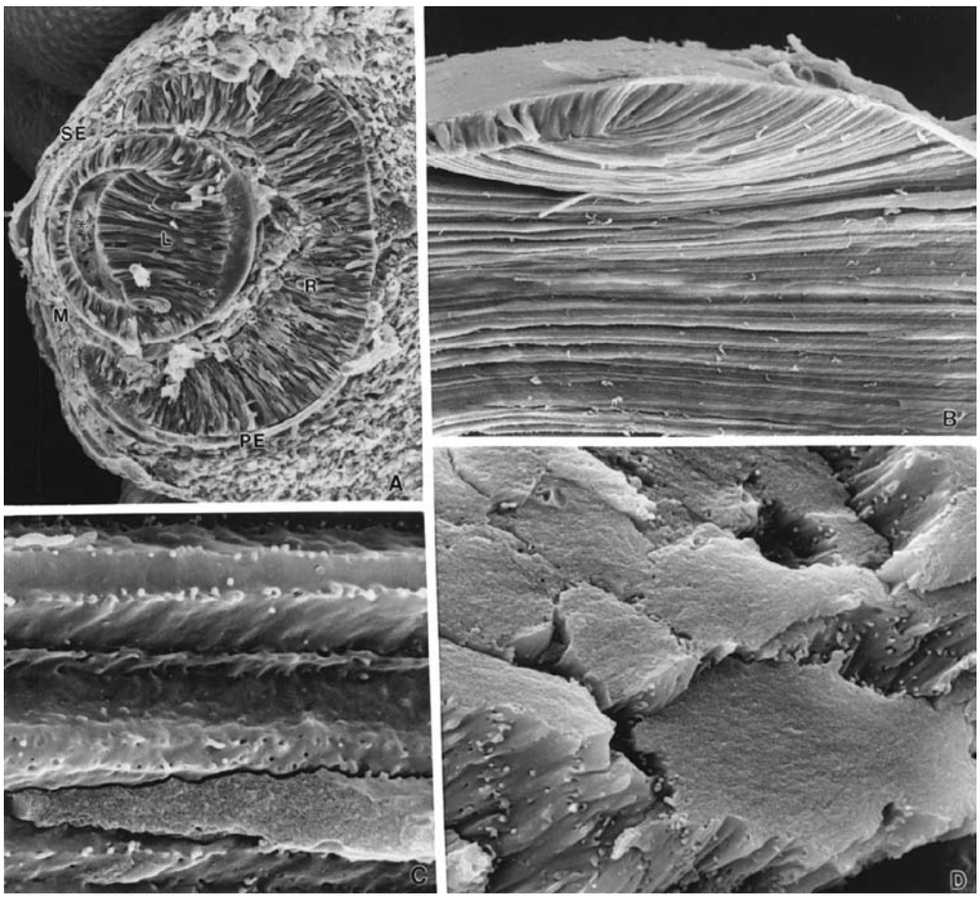

Figure 1.11 **A.** Following detachment of the lens vesicle from the surface ectoderm (SE), the posterior lens epithelial cells–primary lens fibers (L) elongate, obliterating the lens vesicle lumen (equivalent to day 29 of gestation in the dog). Invagination of the optic cup forms the inner neural retina (R) and the outer pigmented epithelium (PE). Mesenchyme of neural crest origin (M) surrounds the optic cup. **B.** Lens bow illustrating elongation of secondary lens fibers. **C** and **D.** Longitudinal view (**C**) and cross-section (**D**) of secondary lens fibers, illustrating the extensive interdigitations and the relative absence of extracellular space. (Reprinted with permission from Sulik, K.K. & Schoenwolf, G.C. (1985) Highlights of craniofacial morphogenesis in mammalian embryos, as revealed by scanning electron microscopy. *Scanning Electron Microscopy*, **4**, 1735–1752.)

cells nearest the presumptive retina, regardless of the orientation of the transplanted lens (Coulombre & Coulombre, 1969). Thus, while the retina develops independently of the lens, the lens appears to be dependent on the retinal primordium for its differentiation. The primitive lens filled with primary lens fibers is the embryonic lens nucleus. In the adult, the embryonic nucleus is the central sphere inside the "Y" sutures; there are no sutures within the embryonal nucleus (Fig. 1.11A, Fig. 1.12, and Fig. 1.13).

At birth, the lens consists almost entirely of lens nucleus, with minimal lens cortex. Lens cortex continues to develop from the anterior cuboidal epithelial cells, which remain mitotic throughout life. Differentiation of epithelial cells into secondary lens fibers occurs at the lens equator (i.e., lens bow; Fig. 1.11B). Lens fiber elongation is accompanied by a corresponding increase in cell volume and a decrease in intercellular space within the lens (Beebe et al., 1982). The lens fibers exhibit a hexagonal cross-sectional shape and extensive surface interdigitations (Fig. 1.11C, D). The secondary lens fibers course anteriorly and posteriorly around the embryonal nucleus to meet at the "Y" sutures (Fig. 1.13).

The zonule fibers are termed the *tertiary vitreous*, but their origin remains uncertain. The zonules may form from the developing ciliary epithelium or the endothelium of the posterior tunica vasculosa lentis (TVL). The embryonic TVL may produce fibrillin-2 and -3, providing a scaffold for zonule formation (Hubmacher et al., 2014). Abnormalities could result in congenital ectopia lentis. Congenitally displaced lenses are often small and are abnormally shaped (i.e., spherophakia), indicating a possible relationship between zonule traction and lens shape. Localized absence of zonules may result in a flattened lens equator; although not a true lens defect, this is often described inaccurately as a lens coloboma (see later Fig. 1.32).

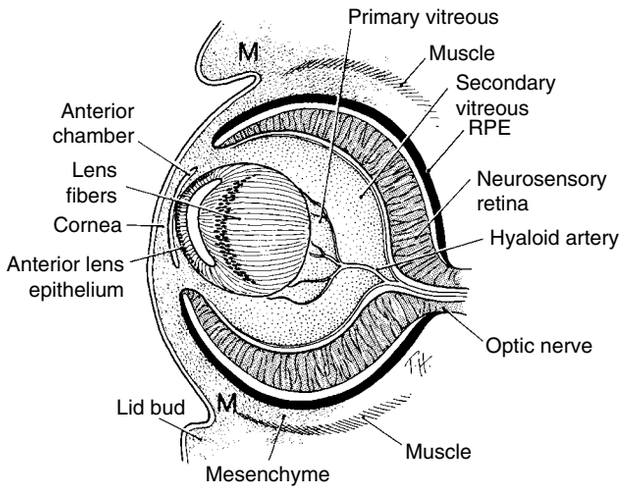

Figure 1.12 Overview of the developing eye surrounded by mesenchyme (M), which is mostly of neural crest origin. The hyaloid vasculature enters the optic cup through the optic fissure and surrounds the lens with capillaries that anastomose with the tunica vasculosa lentis. Axial migration of mesenchyme forms the corneal stroma and endothelium. RPE, retinal pigment epithelium. (Reprinted with permission from Cook, C., Sulik, K.K., & Wright, K.W. (2003) Embryology. In: *Pediatric Ophthalmology and Strabismus* (eds. Wright, K.W. & Spiegel, P.H.), pp. 3–38. New York: Springer.)

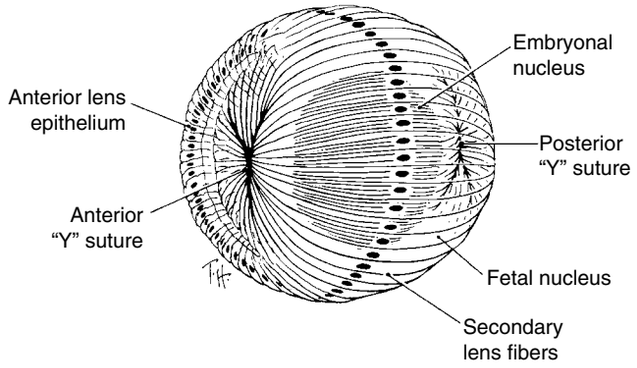

Figure 1.13 Secondary lens fibers and Y sutures. Secondary lens fibers elongate at the equator to span the entire lens, from the anterior to the posterior Y suture. The anterior Y suture is upright; the posterior Y suture is inverted. (Reprinted with permission from Cook, C., Sulik, K.K., & Wright, K.W. (2003) Embryology. In: *Pediatric Ophthalmology and Strabismus* (eds. Wright, K.W. & Spiegel, P.H.), pp. 3–38. New York: Springer.)

Vascular Development

The hyaloid artery is the termination of the primitive ophthalmic artery, a branch of the internal ophthalmic artery, and it remains within the optic cup following closure of the optic fissure. The hyaloid artery branches around the posterior lens capsule and continues anteriorly to anastomose with the network of vessels in the pupillary membrane (Fig. 1.14 and Fig. 1.15A, B; Schaepdrijver et al., 1989). The pupillary membrane consists of vessels and mesenchyme overlying the anterior lens capsule. This hyaloid vascular network that forms around the lens is called the anterior and posterior TVL. The hyaloid artery and associated TVL provide nutrition to the lens and anterior segment during its period of rapid differentiation. Venous drainage occurs via a network near the equatorial lens, in the area where the ciliary body will eventually develop. There is no discrete hyaloid vein (Schaepdrijver et al., 1989).

Once the ciliary body begins actively producing aqueous humor, which circulates and nourishes the lens, the hyaloid system is no longer needed. The hyaloid vasculature and

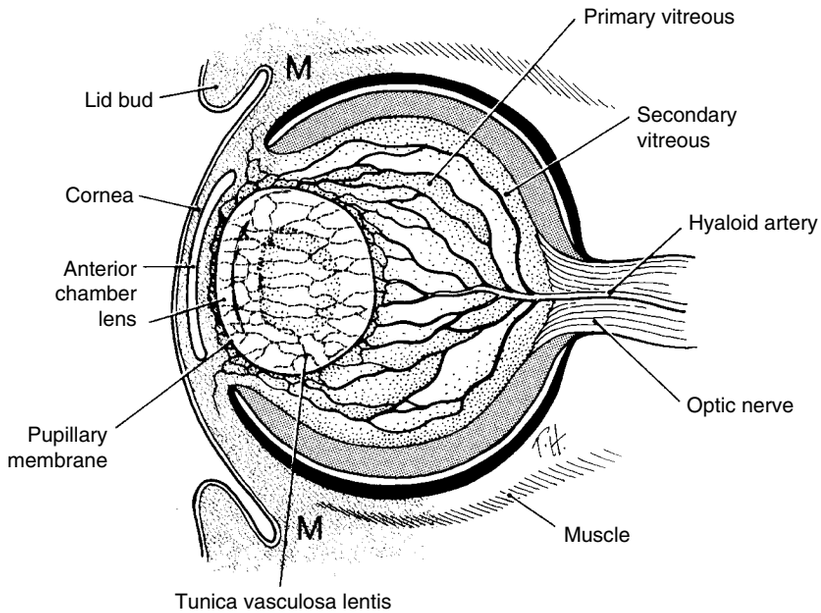

Figure 1.14 The hyaloid vascular system and tunica vasculosa lentis. (Reprinted with permission from Cook, C., Sulik, K.K., & Wright, K.W. (2003) Embryology. In: *Pediatric Ophthalmology and Strabismus* (eds. Wright, K.W. & Spiegel, P.H.), pp. 3–38. New York: Springer.)

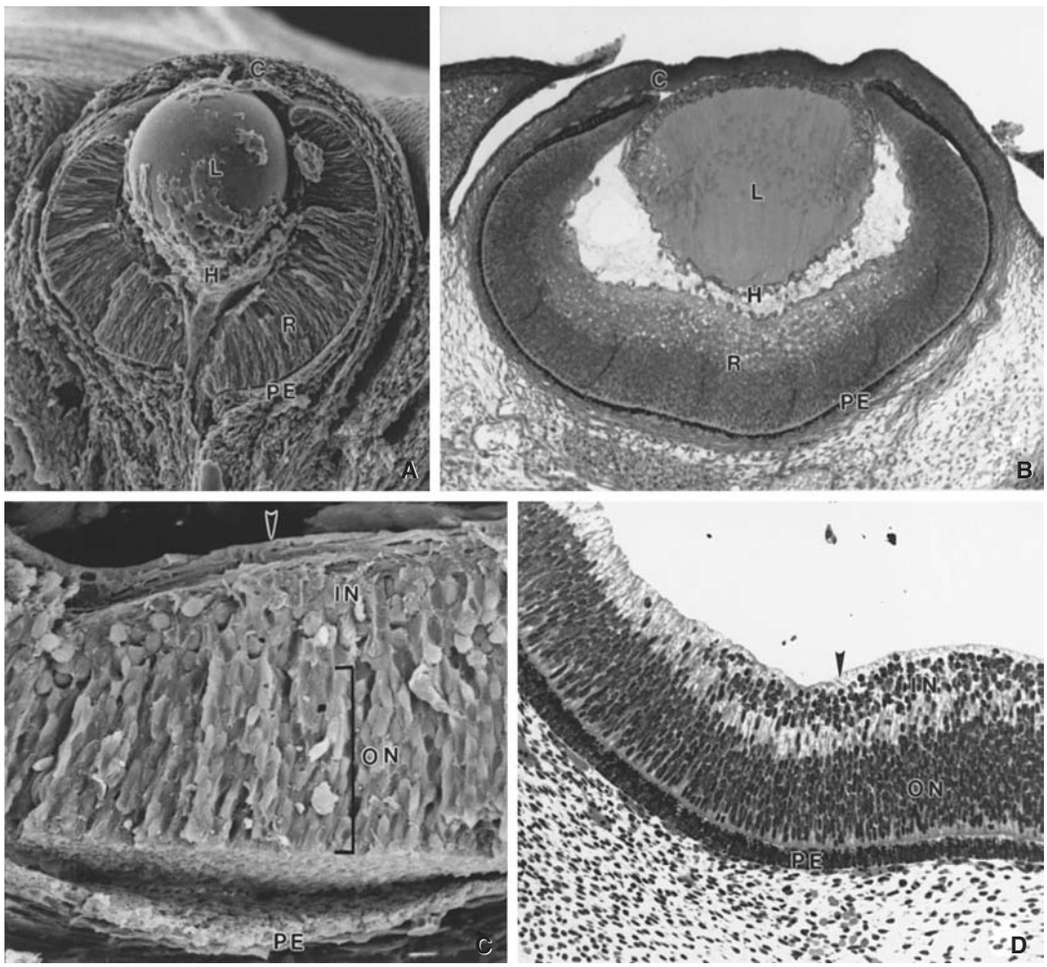

Figure 1.15 **A.** Scanning electron micrograph of a mouse embryo at 14 days of gestation (equivalent to day 32 in the dog). The hyaloid vasculature enters the optic cup through the optic stalk, and it surrounds the lens (L) with capillaries that anastomose with the tunica vasculosa lentis. Axial migration of mesenchyme forms the corneal stroma and endothelium (C). The retina (R) is becoming stratified, whereas the pigment epithelium (PE) remains cuboidal. **B.** The retina becomes stratified into an inner marginal zone and an outer nuclear zone. Note that the inner marginal zone is most prominent in the posterior pole. C, cornea; H, hyaloid artery; L, lens; R, retina. **C.** Segregation of the retina into inner (IN) and outer (ON) neuroblastic layers. The ganglion cells are the first to differentiate, giving rise to the nerve fiber layer (arrowhead). The PE has become artifactually separated in this specimen. **D.** Differentiation of the retina progresses from the central to the peripheral regions. Centrally, the inner (IN) and outer (ON) neuroblastic layers are apparent, with early formation of the nerve fiber layer (arrowhead). Peripherally, however, the retina consists of a single nuclear zone. Between the inner and outer neuroblastic layers is a clear zone, the transient fiber layer of Chievitz. This stage is equivalent to day 32 in the dog. (Panel **A** reprinted with permission from Sulik, K.K. & Schoenwold, G.C. (1985) Highlights of craniofacial morphogenesis in mammalian embryos, as revealed by scanning electron microscopy. *Scanning Electron Microscopy*, **4**, 1735–1752; panel **B** reprinted with permission from Cook, C.S. & Sulik K.K. (1986) Sequential scanning electron microscopic analyses of normal and spontaneously occurring abnormal ocular development in C57B1/6J mice. *Scanning Electron Microscopy*, **3**, 1215–1227; panels **C** and **D** reprinted with permission from Cook, C., Sulik, K.K., & Wright, K.W. (2003) Embryology. In: *Pediatric Ophthalmology and Strabismus* (eds. Wright, K.W. & Spiegel, P.H.), pp. 3–38. New York: Springer.)

TVL reach their maximal development by day 45 in the dog and then begin to regress.

As the peripheral hyaloid vasculature regresses, the retinal vessels develop. Vascular endothelial growth factor (VEGF)-A is a potent angiogenic peptide in the retina; antibody neutralization *in vivo* results in reduction in the hyaloid and retinal vasculature (Feeney et al., 2003). Spindle-shaped mesenchymal cells from the wall of the hyaloid artery at the optic disc form buds (*angiogenesis*) that invade the nerve fiber layer. In contrast, *vasculogenesis* refers to an assembly of dispersed angioblasts into solid cords of mesenchymal cells that later canalize (Fruttiger, 2002; Hughes et al., 2000). Controversy exists as to whether the process of retinal neovascularization occurs primarily through angiogenesis or vasculogenesis (Flower et al., 1985; Fruttiger, 2002; Hughes et al., 2000). Recent studies

indicate that spindle-shaped cells dispersed within the retina, previously thought to be angioblasts, may be immature retinal astrocytes, with retinal vascularization occurring primarily through angiogenesis (Hughes et al., 2000). The primitive capillaries have laminated walls consisting of mitotically active cells secreting basement membrane. Those cells in direct contact with the bloodstream differentiate into endothelial cells; the outer cells become pericytes. Zonulae occludens and gap junctions initially join adjacent cells, but later the capillary endothelium is continuous (Ashton, 1966; Mutlu & Leipold, 1964). The primitive capillary endothelial cells are multipotent and can redifferentiate into fibroblastic, endothelial, or muscle cells, possibly illustrating a common origin for these different tissue types (Ashton, 1966).

Branches of the hyaloid artery become sporadically occluded by macrophages prior to their gradual atrophy (Jack, 1972). Placental growth factor (PlGF) and VEGF appear to be involved in hyaloid regression (Feeney et al., 2003; Martin et al., 2004). Proximal arteriolar vasoconstriction at birth precedes regression of the major hyaloid vasculature (Browning et al., 2001). Atrophy of the pupillary membrane, TVL, and hyaloid artery occurs initially through apoptosis (Ito & Yoshioka, 1999) and later through cellular necrosis (Zhu et al., 2000), and is usually complete by the time of eyelid opening 14 days postnatally.

The clinical lens anomaly known as Mittendorf's dot is a small (1 mm) area of fibrosis on the posterior lens capsule, and it is a manifestation of incomplete regression of the hyaloid artery where it was attached to the posterior lens capsule. Bergmeister's papilla represents a remnant of the hyaloid vasculature consisting of a small, fibrous glial tuft of tissue emanating from the center of the optic nerve. Both are frequently observed as incidental clinical findings.

Development of the Cornea and Anterior Chamber

The anterior margins of the optic cup advance beneath the surface ectoderm and adjacent neural crest mesenchyme after lens vesicle detachment (day 25 in the dog). The surface ectoderm overlying the optic cup (i.e., the presumptive corneal epithelium) secretes a thick matrix, the primary stroma (Hay, 1980; Hay & Revel, 1969). This acellular material consists of collagen fibrils and glycosaminoglycans. Mesenchymal neural crest cells migrate between the surface ectoderm and the optic cup, using the basal lamina of the lens vesicle as a substrate. Proteolysis of collagen IX triggers hydration of the hyaluronic acid, creating the space for cellular migration (Fitch et al., 1998). Initially, this loosely arranged mesenchyme fills the future anterior chamber, and it gives rise to the corneal endothelium and stroma, anterior iris stroma, ciliary muscle, and most structures of the iridocorneal angle (Fig. 1.16A). The presence of an adjacent lens vesicle is required for induction of corneal endothelium, identified by their production of the cell adhesion molecule, n-cadherin (Beebe & Coats, 2000). Type I collagen fibrils and fibronectin secreted by the developing keratocytes form the secondary corneal stroma. Subsequent dehydration results in much of the fibronectin being lost and in a 50% reduction in stromal thickness (Allen et al., 1955; LeDouarin & Teillet, 1974). The endothelium also is important to the dehydration of the stroma. Patches of endothelium become confluent and develop zonulae occludens during days 30–35 in the dog, and during this period Descemet's membrane also forms. The cornea achieves relative transparency at the end of gestation in the dog. Following eyelid opening at approximately 14 days postnatal in the dog, there is an initial decrease in corneal thickness over 4 weeks, presumably as the corneal endothelium become functional. Then, a gradual increase in thickness occurs over the next 6 months (Montiani-Ferreira et al., 2003).

Neural crest migration anterior to the lens to form the corneal stroma and iris stroma also results in formation of a solid sheet of mesenchymal tissue, which ultimately remodels to form the anterior chamber. The portion of this sheet that bridges the future pupil is called the pupillary membrane (Fig. 1.16B, C, and D). Vessels within the pupillary membrane form the TVL, which surrounds and nourishes the lens. These vessels are continuous with those of the primary vitreous (i.e., hyaloid). The vascular endothelium is the only intraocular tissue of mesodermal origin; even the vascular smooth muscle cells and pericytes that originate from mesoderm in the rest of the body are of neural crest origin in the eye (Johnston et al., 1979; Smelser & Ozanics, 1971). In humans, the endothelial lining of Schlemm's canal, like the vascular endothelium elsewhere, is of mesodermal origin. In the dog, atrophy of the pupillary membrane begins by day 45 of gestation and continues during the first two postnatal weeks (Aguirre et al., 1972). Separation of the corneal mesenchyme (neural crest-cell origin) from the lens (surface ectoderm origin) results in formation of the anterior chamber.

In a microphthalmic or nanophthalmic globe, the cornea is correspondingly reduced in diameter. The term *microcornea* is used to describe a cornea that is proportionally smaller than normal for the size of the globe. As with lens induction, determination of the corneal diameter occurs at the time of contact by the optic vesicle with the surface ectoderm. This induction is also sensitive to timing; if the optic vesicle–ectoderm contact occurs earlier or later than normal, the ectoderm may not be fully capable of responding appropriately, resulting in microcornea.

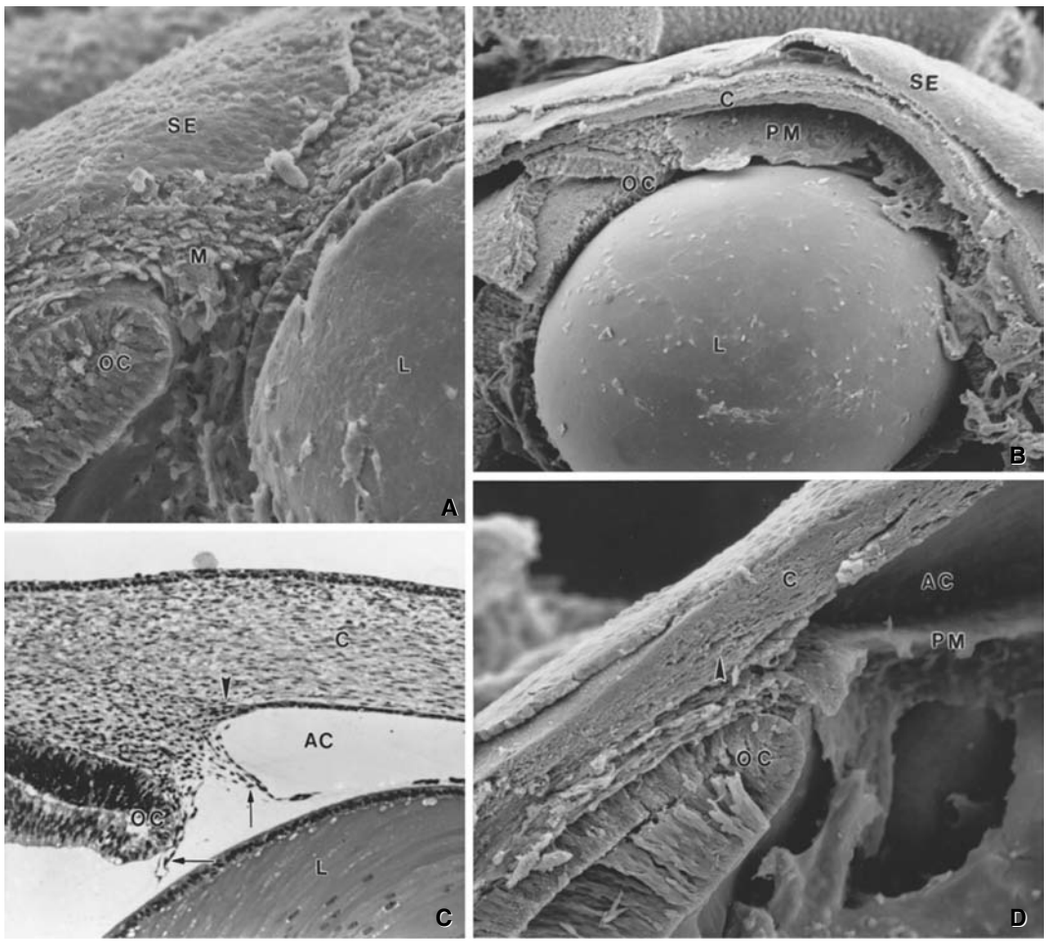

Figure 1.16 **A.** Scanning electron micrograph of a fetal human eye at approximately 42 days of gestation (equivalent to day 25 in the dog). The lens vesicle (L) has detached, and the neural crest–derived mesenchyme (M) is migrating axially between the optic cup (OC) and the surface ectoderm (SE). **B.** On day 54 in the human (day 32 in the dog), the pupillary membrane (PM) is seen within the anterior chamber. The corneal stroma (C) is apparent and is covered by the surface ectoderm (SE), which will become the corneal epithelium. OC, anterior margin of the optic cup, which will form the posterior epithelial layers of the iris, including the pupillary muscles. **C.** Light micrograph obtained at the same stage as in **B** illustrates the pupillary membrane and tunica vasculosa lentis (arrows) originating from the mesenchyme at the margin of the optic cup (OC). The limbal condensation that will become the scleral spur is indicated by the arrowhead. AC, anterior chamber; C, cornea; L, lens. **D.** Scanning electron micrograph of a fetal human eye at approximately 63 days of gestation. The AC is deeper and still bridged by the PM. Endothelialization of clefts within the neural crest–derived corneal stroma (C) by mesoderm will form Schlemm's canal (arrowhead) in the human eye. (Panels **A** and **D** reprinted with permission from Cook, C. (1989) Experimental models of anterior segment dysgenesis. *Ophthalmic Paediatrics and Genetics*, **10**, 33–46; panels **B** and **C** reprinted with permission from Cook, C., Sulik, K.K., & Wright, K.W. (2003) Embryology. In: *Pediatric Ophthalmology and Strabismus* (eds. Wright, K.W. & Spiegel, P.H.), pp. 3–38. New York: Springer.)

Development of the Iris, Ciliary Body, and Iridocorneal Angle

The two layers of the optic cup (neuroectoderm origin) consist of an inner, nonpigmented layer and an outer, pigmented layer. Both the pigmented and nonpigmented epithelium of the iris and the ciliary body develop from the anterior aspect of the optic cup; the retina develops from the posterior optic cup. The optic vesicle is organized with all cell apices directed to the center of the vesicle. During optic cup invagination, the apices of the inner and outer epithelial layers become adjacent. Thus, the cells of the optic cup are oriented apex to apex.

A thin, periodic acid–Schiff-positive basal lamina lines the inner aspect (i.e., vitreous side) of the nonpigmented epithelium and retina (i.e., inner limiting membrane). By approximately day 40 of gestation in the dog, both the pigmented and nonpigmented epithelial cells show apical cilia that project into the intercellular space. There also is increased prominence of Golgi complexes and associated vesicles within the ciliary epithelial cells. These changes, as well as the presence of "ciliary channels" between the

apical surfaces, probably represent the first production of aqueous humor.

The iris stroma develops from the anterior segment mesenchymal tissue (neural-crest cell origin), and the iris pigmented and nonpigmented epithelium originate from the neural ectoderm of the optic cup. The smooth muscle of the pupillary sphincter and dilator muscles ultimately differentiate from these epithelial layers, and they represent the only mammalian muscles of neural ectodermal origin. In avian species, however, the skeletal muscle cells in the iris are of neural crest origin, with a possible small contribution of mesoderm to the ventral portion (Nakano & Nakamura, 1985; Yamashita & Sohal, 1986, 1987).

Differential growth of the optic cup epithelial layers results in folding of the inner layer, representing early anterior ciliary processes (Fig. 1.16B). The ciliary body epithelium develops from the neuroectoderm of the anterior optic cup, and the underlying mesenchyme differentiates into the ciliary muscles. Extracellular matrix secreted by the ciliary epithelium becomes the tertiary vitreous and, ultimately, is thought to develop into lens zonules.

Three phases of iridocorneal angle maturation have been described (Reme et al., 1983a, 1983b). First is separation of anterior mesenchyme into corneoscleral and iridociliary regions (i.e., trabecular primordium formation), followed by differentiation of ciliary muscle and folding of the neural ectoderm into ciliary processes. Second is enlargement of the corneal trabeculae and development of clefts in the area of the trabecular meshwork, which is accompanied by regression of the corneal endothelium covering the angle recess. Third is postnatal remodeling of the drainage angle, associated with cellular necrosis and phagocytosis by macrophages, resulting in opening of clefts in the trabecular meshwork and outflow pathways.

This change in the relationship of the trabecular meshwork to the ciliary body and iris root during the last trimester of human gestation occurs through differential growth, with posterior movement of the iris and the ciliary body relative to the trabecular meshwork exposing the outflow pathways. This results in progressive deepening of the chamber angle and normal conformation of the ciliary muscle and ciliary processes (Anderson, 1981). This is in contrast to previous theories of cleavage of the iris root from the cornea or atrophy of angle tissue (Barishak, 1978; Smelser & Ozanics, 1971; Wulle, 1972).

In species born with congenitally fused eyelids (i.e., dog and cat), development of the anterior chamber continues during this postnatal period before eyelid opening. At birth, the peripheral iris and cornea are in contact. Maturation of pectinate ligaments begins by 3 weeks postnatal and rarefaction of the uveal and corneoscleral trabecular meshworks to their adult state occurs during the first 8 weeks after birth. There is no evidence of mesenchymal splitting, cell death, or phagocytic activity (Samuelson & Gelatt, 1984a, 1984b).

Retina and Optic Nerve Development

Infolding of the neuroectodermal optic vesicle results in a bilayered optic cup with the apices of these two cell layers in direct contact. Primitive optic vesicle cells are columnar, but by 20 days of gestation in the dog, they form an outer cuboidal layer containing the first melanin granules in the developing embryo within the future retinal pigment epithelium (RPE). The neurosensory retina develops from the inner, nonpigmented layer of the optic cup, and the RPE originates from the outer, pigmented layer. Bruch's membrane (the basal lamina of the RPE) is first seen during this time, and becomes well developed over the next week, when the choriocapillaris is developing. By day 45 in the dog, the RPE cells take on a hexagonal cross-sectional shape and develop microvilli that interdigitate with projections from photoreceptors of the nonpigmented (inner) layer of the optic cup.

At the time of lens placode induction, the retinal primordium consists of an outer, nuclear zone and an inner, marginal (anuclear) zone. Cell proliferation occurs in the nuclear zone, with migration of cells into the marginal zone. This process forms the inner and outer neuroblastic layers, separated by their cell processes that make up the transient fiber layer of Chievitz (Fig. 1.15C, D). Cellular differentiation progresses from inner to outer layers and, regionally, from central to peripheral locations. Peripheral retinal differentiation may lag behind that occurring in the central retina by 3–8 days in the dog (Aguirre et al., 1972). Retinal histiogenesis beyond formation of the neuroblastic layers requires induction by a differentiated RPE. There are several rodent models of RPE dysplasia resulting in failure of later retinal differentiation and subsequent degeneration (Bumsted & Barnstable, 2000; Cook et al., 1991b). Retinal ganglion cells develop first within the inner neuroblastic layer, and axons of the ganglion cells collectively form the optic nerve. Cell bodies of the Müller and amacrine cells differentiate in the inner portion of the outer neuroblastic layer. Horizontal cells are found in the middle of this layer; the bipolar cells and photoreceptors mature last, in the outermost zone of the retina (Greiner & Weidman, 1980, 1981, 1982; Spira & Hollenberg, 1973).

Significant retinal differentiation continues postnatally, particularly in species born with fused eyelids. Expression of extracellular matrix elements, chondroitin sulfate, and heparin sulfate occurs in a spatiotemporally regulated manner, with a peak of chondroitin sulfate occurring at the time of eyelid opening, This corresponds to the period of photoreceptor differentiation (Erlich et al., 2003). At birth, the canine retina has reached a stage of development equivalent to the human at 3–4 months of gestation (Shively et al., 1971). In the kitten, all ganglion cells and central retinal cells are present at birth, with continued proliferation in the peripheral retina continuing during the first 2–3 postnatal weeks in dogs and cats (Johns et al., 1979; Shively et al., 1971).

Possible means of retinal regeneration have become reality with the discovery of neural stem cells in the mature eye of warm-blooded vertebrates (Engelhardt et al., 2004; Fischer, 2005). These include cells at the retinal margin, pigmented cells in the ciliary body and iris, nonpigmented cells in the ciliary body, and Müller glia within the retina. Under the influence of growth factors, these neuroectodermal cells in the avian are capable of undergoing differentiation into retinal cells (Fischer, 2005).

Sclera, Choroid, and Tapetum

These neural crest–derived tissues are all induced by the outer layer of the optic cup (future RPE). Normal RPE differentiation is a prerequisite for normal development of the sclera and choroid. The choroid and sclera are relatively differentiated at birth, but the tapetum in dogs and cats continues to develop and mature during the first 4 months postnatally. The initially mottled, blue appearance of the immature tapetum is replaced by the blue/green to yellow/orange color of the adult. These color variations seen in immature dogs can prove a challenge to accurate funduscopic assessment.

Posterior segment uveoscleral colobomas most often result from a primary RPE abnormality. Subalbinotic animals have a higher incidence of posterior segment colobomas, with reduced RPE pigmentation being a marker for abnormal RPE development (Bertram et al., 1984; Cook et al., 1991a; Gelatt & McGill, 1973; Gelatt & Veith, 1970; Munyard et al., 2007; Rubin et al., 1991). The most common example is the choroidal hypoplasia of Collie eye anomaly (Barnett, 1979).

Vitreous

The primary vitreous forms posteriorly, between the primitive lens and the inner layer of the optic cup (see Fig. 1.10 and Fig. 1.12). In addition to the vessels of the hyaloid system, the primary vitreous also contains mesenchymal cells, collagenous fibrillar material, and macrophages. The secondary vitreous forms as the fetal fissure closes, and contains a matrix of cellular and fibrillar material, including primitive hyalocytes, monocytes, and hyaluronic acid (Akiya et al., 1986; Bremer & Rasquin, 1998). Identification of microscopic vascular remnants throughout the vitreous of adult rabbits has led to speculation for interactive remodeling of the primary vitreous to form secondary vitreous (Los et al., 2000a, 2000b). Plasma proteins enter and leave the vitreous and, in the chick, there is a concentration of 13% of that found in plasma, until a decline to 4% of plasma levels occurs during the last week prior to hatching (Beebe et al., 1986). Primitive hyalocytes produce collagen fibrils that expand the volume of the secondary vitreous.

The tertiary vitreous forms as a thick accumulation of collagen fibers between the lens equator and the optic cup. These fibers are called the marginal bundle of Drualt or Drualt's bundle. Drualt's bundle has a strong attachment to the inner layer of the optic cup, and it is the precursor to the vitreous base and lens zonules. The early lens zonular fibers appear to be continuous with the inner, limiting membrane of the nonpigmented epithelial layer covering the ciliary muscle. Elastin and emulin (elastin microfibril interface located protein) have been identified in developing zonules and Descemet's membrane (Bressan et al., 1993; Horrigan et al., 1992). Experimental exposure of chick embryos to homocysteine results in deficient zonule development and congenital lens luxation (Maestro De Las Casas et al., 2003). Traction of the zonules contributes to expansion of the lens and localized absence of zonules can lead to a corresponding area of the lens that is flattened and inaccurately referred to as a lens coloboma (see later Fig. 1.32).

Atrophy of the primary vitreous and hyaloid leaves a clear, narrow central zone, which is called Cloquet's canal. In the mouse, Doppler ultrasound biomicroscopy has been used to document *in vivo* the decrease in blood velocity associated with hyaloid regression between birth and postnatal day 13 (Brown et al., 2005). Most of the posterior vitreous gel at birth is secondary vitreous, with the vitreous base and zonules representing tertiary vitreous.

Optic Nerve

Axons from the developing ganglion cells pass through vacuolated cells from the inner wall of the optic stalk. A glial sheath forms around the hyaloid artery. As the hyaloid artery regresses, the space between the hyaloid artery and the glial sheath enlarges. Bergmeister's papilla represents a remnant of these glial cells around the hyaloid artery. Glial cells migrate into the optic nerve and form the primitive optic disc. The glial cells around the optic nerve and the glial part of the lamina cribrosa come from the inner layer of the optic stalk, which is of neural ectoderm origin. Later, a mesenchymal (neural crest origin) portion of the lamina cribrosa develops. Myelinization of the optic nerve begins at the chiasm, progresses toward the eye, and reaches the optic disc after birth.

Eyelids

The eyelids develop from surface ectoderm, which gives rise to the epidermis, cilia, and conjunctival epithelium. Neural crest mesenchyme gives rise to deeper structures, including the dermis and tarsus. The eyelid muscles (i.e., orbicularis and levator) are derived from craniofacial condensations of mesoderm called somitomeres. In the craniofacial region, presumptive connective tissue–forming mesenchyme derived from the neural crest imparts spatial patterning information

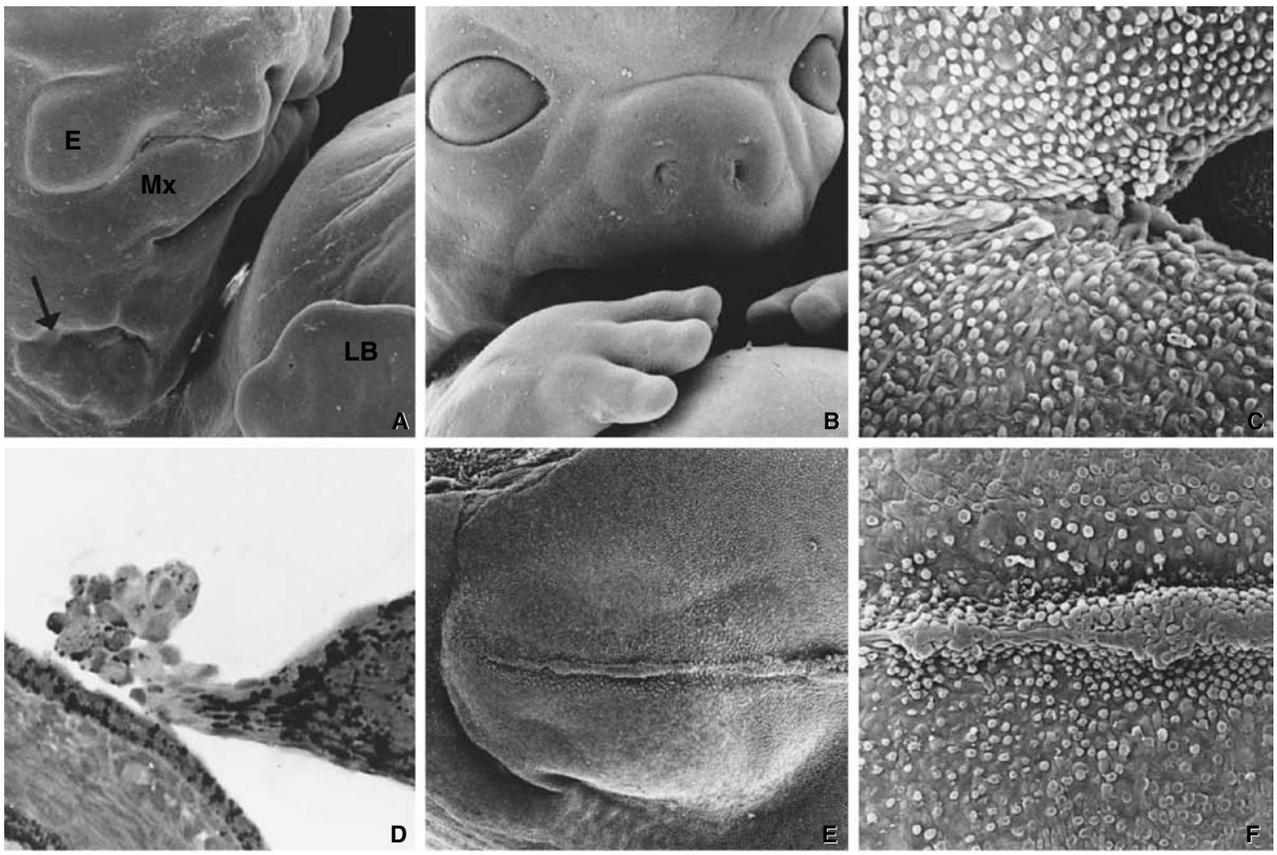

Figure 1.17 **A.** Lateral view of the head of a human embryo at 6 weeks of gestation. The individual hillocks that will form the external ear can be identified both cranial and caudal to the first visceral groove (arrow). The developing eye is adjacent to the maxillary prominence (Mx). LB, forelimb bud. **B.** Frontal view of the head of a human embryo at 8 weeks of gestation. Formation of the face is largely complete, and the eyelids are beginning to close. **C.** Eyelid closure begins at the medial and lateral canthi and progresses axially. **D.** Light micrograph of the eyelid marginal epithelium in a mouse at day 15 of gestation. The actively migrating epithelium forms a cluster of cells adjacent to the corneal epithelium. **E** and **F.** Surface view of the fused eyelids from a human embryo at 10 weeks of gestation. (Panels **A**, **B**, **E**, and **F** reprinted with permission from Sulik, K.K. & Schoenwolf G.C. (1985) Highlights of craniofacial morphogenesis in mammalian embryos, as revealed by scanning electron microscopy. *Scanning Electron Microscopy*, **4**, 1735–1752; panel **D** reprinted with permission from Cook, C.S. & Sulik, K.K. (1986) Sequential scanning electron microscopic analyses of normal and spontaneously occurring abnormal ocular development in C57B1/6J mice. *Scanning Electron Microscopy*, **3**, 1215–1227.)

upon myogenic cells that invade it (Noden, 1986). The upper eyelid develops from the frontonasal process; the lower eyelid develops from the maxillary process. The lid folds grow together and elongate to cover the developing eye (Fig. 1.17). The upper and lower lids fuse on day 32 of gestation in the dog. Separation occurs 2 weeks postnatally.

Extraocular Muscles

The extraocular muscles arise from mesoderm in somitomeres (i.e., preoptic mesodermal condensations; Jacobson, 1988; Meier, 1982; Meier & Tam, 1982; Packard & Meier, 1983; Tam, 1986; Tam et al., 1982; Tam & Trainor, 1994; Trainor & Tam, 1995). Spatial organization of developing eye muscles is initiated before they interact with the neural crest mesenchyme. Patterning of the segmental somitomeres follows that of the neural crest; that is, somitomere I (forebrain), somitomere III (caudal midbrain), and somitomeres IV and VI (hindbrain; Trainor & Tam, 1995). From studies of chick embryos, it has been shown that the oculomotor-innervated muscles originate from the first and second somitomeres, the superior oblique muscle from the third somitomere, and the lateral rectus muscle from the fourth somitomere (Wahl et al., 1994). The entire length of these muscles appears to develop spontaneously rather than from the orbital apex anteriorly, as had been previously postulated (Sevel, 1981, 1986). Congenital extraocular muscle abnormalities are rarely identified and reported in the dog (Martin, 1978). This may be a result of several factors, including the fact that the extraocular muscles are normally less well developed in domestic mammals compared with humans,

and the limited ability to assess minor abnormalities which would be manifest as impaired binocular vision.

Developmental Ocular Anomalies

Cyclopia and Synophthalmia

Formation of a single median globe (i.e., cyclopia) or two incompletely separated or fused globes (i.e., synophthalmia) may occur by two different mechanisms. The "fate maps," which have been produced for amphibian embryos, have revealed the original location of the neural ectodermal tissue that will form the globes as a single, bilobed area crossing the midline in the anterior third of the trilaminar embryonic disc. An early defect in separation of this single field could result in the formation of a single, or incompletely separated, median globe(s) (Fig 1.18A). After separation into bilateral optic vesicles, later loss of the midline territory in the embryo could result in fusion of the ocular fields. This loss of midline territory, prior to separation into two eye fields, is seen in holoprosencephaly, and the facial features characteristic of human fetal alcohol syndrome represent a mild end of the holoprosencephalic spectrum (Cohen & Sulik, 1992; Sulik & Johnston, 1982). Cases of cyclopia or synophthalmia are invariably associated with severe craniofacial malformations (Fig. 1.18A and B) and are usually nonviable.

Cyclopia is rarely identified in dogs (Njoku et al., 1978). However, in sheep, ingestion of the alkaloids (cyclopamine and jervine) from the weed *Veratrum californicum* by pregnant ewes on day 14 of gestation (total duration of gestation 150 days) is the best-documented example of teratogen-induced cyclopia and synophthalmia in domestic animals (Binns et al., 1959; Bryden et al., 1971; Cooper et al., 1998; Incardona et al., 1998; Keeler, 1990; Keeler & Binns, 1966; Saperstein, 1975). It has been shown that cyclopamine specifically blocks the Sonic hedgehog (Shh) signaling pathway (Cooper et al., 1998; Incardona et al., 1998, 2000). The specific timing for veratrum-induced cyclopia in sheep corresponds to the period of gastrulation and formation of the neural plate before separation of the optic fields. Exposure to the alkaloid earlier in gestation results in fetal death; later exposure causes skeletal malformation or has no effect, thus demonstrating the importance of narrow, sensitive periods in development.

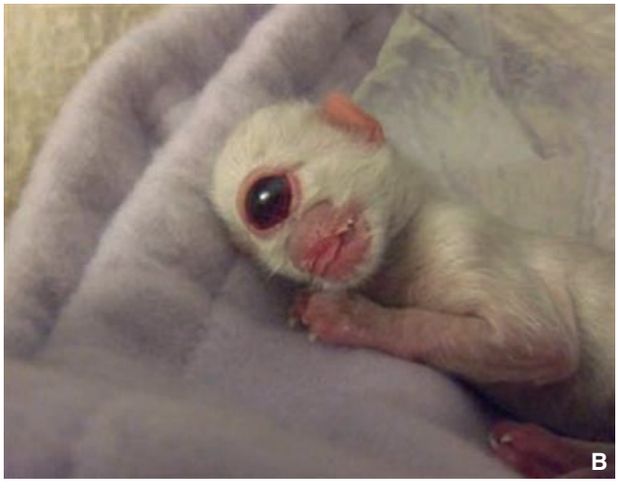

Figure 1.18 **A.** Cyclopia in a Holstein calf, etiology unknown. Note the single median globe, palpebral fissure, cornea, and pupil. **B.** Cyclopia in a nonviable kitten. Note the narrow forebrain and midface regions. The limbs and axial skeleton are relatively normal, demonstrating limited effect on the forebrain region of the embryo. (Panel **A** courtesy of Brian Wilcock.)

Microphthalmia and Anophthalmia

Microphthalmia can occur early in development through a deficiency in the optic vesicle (Fig. 1.19A), or later through failure of normal growth and expansion of the optic cup (Fig. 1.19B). An early deficiency in the size of the globe as a

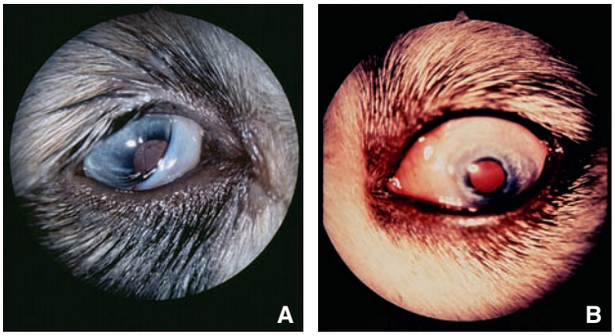

Figure 1.19 **A.** Microphthalmia and persistent pupillary membranes in a Chow Chow puppy. Note that the size of the palpebral fissure is proportional to the reduced size of the globe as a whole. This is consistent with microphthalmia induced at the optic vesicle stage. **B.** Microphthalmia induced at a later stage of gestation, possibly by delayed closure of the optic fissure, although this eye does not exhibit a coloboma. Note the larger size of the palpebral fissure relative to the small globe.

whole is often associated with a correspondingly small, palpebral fissure. The fissure size is determined by the optic vesicle size during its contact with the surface ectoderm, so this supports a malformation sequence beginning at formation of the optic sulcus, optic vesicle, or earlier. Results from studies of teratogen-induced ocular malformations have been helpful in identifying sensitive developmental periods. Acute exposure to teratogens before optic sulcus formation results in an overall deficiency of the neural plate, with subsequent reduction in the optic vesicle size. When microphthalmia originates during development of the neural plate/optic sulcus, it is often associated with multiple ocular malformations, including anterior segment dysgenesis, cataract, retinal dysplasia, and persistence of the hyaloid (Table 1.3).

Later initiation of microphthalmia can occur through failure to establish early IOP (Berman & Pierro, 1969; Hero et al., 1991). Placement of a capillary tube into the vitreous cavity of the embryonic chick eye reduces the IOP and markedly slows growth of the eye (Coulombre, 1956). Histologic examination of the intubated eyes demonstrates a proportional reduction in the size of all ocular tissues except the neural retina and the lens, which are normal in size for the age of the eye. The retina in these eyes is highly convoluted, filling the small posterior segment. Thus, it has been concluded that growth of the neural retina occurs independent of the other ocular tissues. Experimental removal of the lens does not alter retinal growth (Coulombre & Coulombre, 1964). Growth of the choroid and sclera appears to depend on IOP, as does folding of the ciliary epithelium (Bard et al., 1975; Cook, 1989, 1995; Cook & Sulik, 1988). Thus, failure of fusion of the optic fissure can result in microphthalmia and associated malformations (i.e., colobomatous microphthalmia). A delay in closure of this fissure during a critical growth period may result in inadequate globe expansion as well. If the fissure eventually closes, however, it may be difficult to distinguish between colobomatous and noncolobomatous microphthalmia. If the optic vesicle develops normally before abnormal (delayed) closure of the optic fissure, the palpebral fissure may not be reduced in size as much as the globe as a whole is reduced (Fig. 1.19B). In most cases, microphthalmia occurs through a combination of cellular deficiency within the optic vesicle/cup compounded by failure of the optic fissure to close on schedule.

Table 1.3 Anomalies associated with microphthalmia in dogs.

Anomaly	Breed	References
Anterior segment dysgenesis	Saint Bernard, Doberman	Arnbjerg & Jensen (1982); Bergsjo et al. (1984); Boroffka et al. (1998); Lewis et al. (1986); Martin & Leipold (1974); Peiffer & Fischer (1983); Stades (1980, 1983); van der Linde-Sipman et al. (1983)
Cataract	Old English Sheepdog	Barrie et al. (1979)
	Akita	Laratta et al. (1985)
	Miniature Schnauzer	Gelatt et al. (1983); Samuelson et al. (1987); Zhang et al. (1991)
	Chow Chow	Collins et al. (1992)
	Cavalier King Charles Spaniel	Narfstrom & Dubielzig (1984)
	English Cocker Spaniel	Strande et al. (1988)
	Irish Wolfhound	Kern (1981)
Retinal dysplasia	Saint Bernard	Martin & Leipold (1974)
	Doberman	Arnbjerg & Jensen (1982); Bergsjo et al. (1984); Lewis et al. (1986); Peiffer & Fischer (1983)

Anophthalmia represents an extreme on the spectrum of microphthalmia. In most cases, careful examination of the orbital contents will reveal primitive ocular tissue (i.e., actual microphthalmia). True anophthalmia results from a severe developmental deficiency in the primitive forebrain, at a stage before optic sulcus formation. This usually results in a nonviable fetus.

Microphthalmia in domestic animals occurs sporadically and is associated with multiple malformations (Table 1.3), including anterior segment dysgenesis, cataract, persistent hyperplastic primary vitreous (Bayon et al., 2001; Boeve et al., 1992; van der Linde-Sipman et al., 1983), and retinal dysplasia (Bayon et al., 2001; Bertram et al., 1984). In the Doberman Pinscher, microphthalmia, anterior segment dysgenesis, and retinal dysplasia are thought to be inherited as autosomal recessive traits (Bergsjo et al., 1984). Inherited microphthalmia in Texel sheep has as its primary event abnormal development with involution of the lens vesicle followed by proliferation of dysplastic mesenchyme, which develops into cartilage, smooth muscle, fat, and lacrimal gland (van der Linde-Sipman et al., 2003).

A similar spectrum of multiple ocular malformations has been described as a presumably inherited condition associated with central nervous system malformations in Angus (Rupp & Knight, 1984), Shorthorn (Greene & Leipold, 1974), and Hereford cattle (Blackwell & Cobb, 1959; Kaswan et al., 1987), as well as in nondomestic species, including raptors (Buyukmihci et al., 1988), camel (Moore et al., 1999), and white-tailed deer (Wyand et al., 1972). Colobomatous microphthalmia is initiated later in gestation.

In swine, congenital microphthalmia has been historically reported to be associated with maternal vitamin A deficiency (Hale, 1935; Manoly, 1951; Roberts, 1948). Conversely, maternal excess of vitamin A and its analogue, retinoic acid, has been demonstrated (Bayon et al., 2001) to result

in teratogenic ocular and craniofacial malformations in humans and laboratory animals (Cook, 1989; Cook & Sulik, 1988, 1990; Mulder et al., 2000).

Colobomatous Malformations

A coloboma refers broadly to any congenital (present at birth) tissue defect. Ocular colobomas most frequently involve the vascular tunic of the eye, namely the iris and choroid. The spectrum encompasses minor defects (i.e., dyscoria) as well as major defects (i.e., aniridia). Aniridia occurs rarely in animals (Irby & Aguirre, 1985; Saunders & Fincher, 1951), but is seen as a malformation in humans associated with genetic syndromes including Rieger syndrome (*PITX2* gene; Perveen et al., 2000) and *PAX6* gene mutations (Sonoda et al., 2000). The iris stroma develops from neural crest mesenchyme induced by the bilayered epithelium of the anterior optic cup. Thus, a complete and full-thickness defect in the iris most likely results from incomplete axial expansion of the anterior optic cup. Iris hypoplasia represents the mild spectrum of this type of coloboma and is seen frequently in dogs (particularly those breeds characterized by subalbinism) and has been recognized as a genetic syndrome in horses (Ewart et al., 2000).

The classic explanation for localized colobomatous malformations involves failure of the optic fissure to close. Such failure may result in secondary "colobomatous" microphthalmia (Fig. 1.20) and, in experimental models, there may be deviation of the fissure by 90° or more. When defects are located in any inferior location (particularly in a small globe), this is the most likely explanation. This defect in closure of the optic fissure (future RPE and ciliary and iris epithelium) results in failure of induction of the adjacent choroid and sclera. Any or all of these layers may be affected. The clinically apparent sequella to abnormal fissure closure may be only a subtle degree of dyscoria (Matsuura et al., 2013).

Figure 1.20 Microphthalmia and an inferior coloboma of the scleral and uveal tissue allowing vitreous prolapse into the subconjunctival space. In colobomatous microphthalmia, globe expansion is impaired by the inability to establish intraocular pressure because of the optic fissure failing to close. Both mechanisms of microphthalmia may occur in a single eye.

Many colobomatous defects, however, occur in other locations (Briziarelli & Abrutyn, 1975; Gelatt et al., 1969; Gwin et al., 1981). Differentiation of the neural crest–derived stroma of the choroid and iris is determined by the adjacent structures of the outer layer of the optic cup: anteriorly the iris and ciliary epithelium, and posteriorly the RPE. In sequential analyses of animals exhibiting primary abnormalities in differentiation of the outer layer of the optic cup, anterior and posterior segment colobomas are associated with uveal epithelium/RPE defects (Cook et al., 1991a, 1991b; Zhao & Overbeek, 2001).

Prenatal studies of colobomas in the Australian Shepherd dog have demonstrated a primary defect in the RPE, resulting in hypoplasia of the adjacent choroid and sclera (Fig. 1.21 and Fig. 1.22; Cook et al., 1991a). This condition is referred to as merle ocular dysgenesis (MOD) because of the correlation with the merle coat coloration (Bertram et al., 1984). A similar spectrum has been identified in cattle (Gelatt et al., 1969), Great Dane dogs, and cats (Gwin et al., 1981) exhibiting incomplete albinism. It is likely that the subalbinism is associated with abnormal RPE that fails to induce the overlying neural crest.

Choroidal hypoplasia in the Collie dog (i.e., "Collie eye anomaly" or CEA; Barnett, 1979) may represent a malformation sequence similar to that of MOD (Fig. 1.23 and Fig. 1.24). Differences between CEA and MOD are illustrated in Table 1.4. CEA has been widely described in the Collie, Border Collie, Shetland Sheepdog, and Australian Shepherd (Barnett, 1979; Barnett & Stades, 1979; Bedford, 1982a; Rubin et al., 1991). Variations of this congenital malformation, including scleral ectasia, sporadically occur in other breeds as well (Bedford, 1998). It has been demonstrated that choroidal hypoplasia associated with CEA segregates as an autosomal recessive trait with nearly 100% penetrance (Lowe et al., 2003).

Optic nerve coloboma as an isolated finding is likely caused by localized failure of closure of the optic fissure that begins to close at the level of the disc with progression anterior and posterior. Optic nerve coloboma is seen unassociated with genetically identifiable CEA mutation NHEJ1 in the Nova Scotia Duck Tolling Retriever (Brown et al., 2018).

Dermoid

The presence of aberrant tissue (e.g., skin, cartilage, bone) within the orbit may originate early in development through abnormal differentiation of an isolated group of cells. Arrest or inclusions of epidermal and connective tissues (i.e., surface ectoderm and neural crest) may occur during closure of

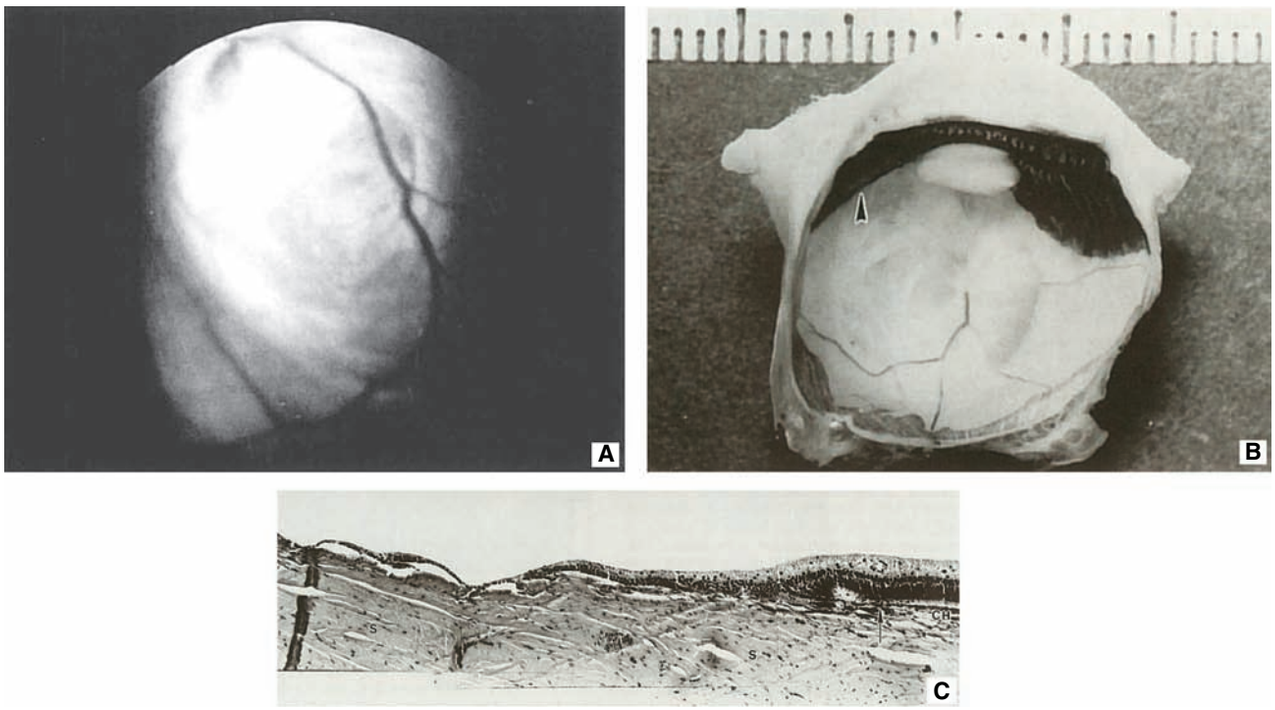

Figure 1.21 Clinical (**A**) and gross (**B**) photographs of the ocular fundus of an adult Australian Shepherd dog affected with merle ocular dysgenesis. Note the large excavation of the equatorial posterior segment. There is also a defect in the ciliary body (arrowhead), which was not apparent clinically. **C.** At the light microscopic level, defects such as this consist of a thin layer of sclera (S) lined by a glial membrane. Note the abrupt transition from normal retina, retinal pigment epithelium (RPE), and choroid seen on the right to the sudden loss of RPE and choroid at the level indicated by the arrow. (Reprinted with permission from Cook, C., Burling, K., & Nelson E. (1991) Embryogenesis of posterior segment colobomas in the Australian Shepherd dog. *Progress in Veterinary & Comparative Ophthalmology*, **1**, 163–170.)

the fetal clefts. Abnormal invagination of ectodermal tissue later in gestation may result in a pocket of well-differentiated dermal tissue. Eyelid dermoids may occur though isolation of an island of ectoderm later forming a nodule of tissue that is, strictly speaking, not abnormal in location, but in configuration, a nonneoplastic overgrowth of tissue disordered in structure (Fig. 1.25). These are termed *hamartomas* (i.e., benign tissue mass resulting from faulty development). Limbal dermoids represent *choristomas* (i.e., mass formed by tissue not normally found at this site; Fig. 1.26). Both eyelid epidermis and corneal epithelium originate from surface ectoderm, following induction by the optic vesicle, and there appears to be a narrow period during which the surface ectoderm can respond to inductive influences to produce a normal lens. The same may be true for induction of the cornea. Dermoids are seen in all species as an incidental finding, and they are seen as an inherited condition in cattle and some dog breeds (Adams et al., 1983; Barkyoumb & Leipold, 1984).

Anterior Segment Dysgenesis

The anterior segment dysgeneses identified in humans encompass a broad range of malformations, including Peters' anomaly, Axenfeld–Rieger syndrome, iridocorneal endothelium syndrome, posterior polymorphous dystrophy, and Sturge–Weber syndrome. Similar anomalies have been described in domestic animals, generally as sporadic occurrences (Irby & Aguirre, 1985; Peiffer, 1982; Rebhun, 1977; Swanson et al., 2001). Anterior segment dysgenesis is often associated with microphthalmia (Arnbjerg & Jensen, 1982; Bergsjo et al., 1984; Lewis et al., 1986; Martin & Leipold, 1974; Peiffer & Fischer, 1983).

In domestic animals, *persistent pupillary membranes* represent the most common manifestation of anterior segment dysgenesis. In the embryo, the pupillary membrane forms a solid sheet of tissue that is continuous with the iris at the level of the collarette (see Fig. 1.19). Regression occurs during the first two postnatal weeks, before eyelid opening in the dog. Persistence of some pupillary membrane strands was noted in 0.7% of 575 Beagles aged from 16 to 24 weeks (Bellhorn, 1974). Inherited persistent pupillary membranes occur in the Basenji dog (Bistner et al., 1971; Roberts & Bistner, 1968), and they may be associated with corneal or lens opacities (or both) at the site of membrane attachments. Complete persistence of a sheet of tissue bridging the pupil is rare and results in visual impairment. Persistent pupillary

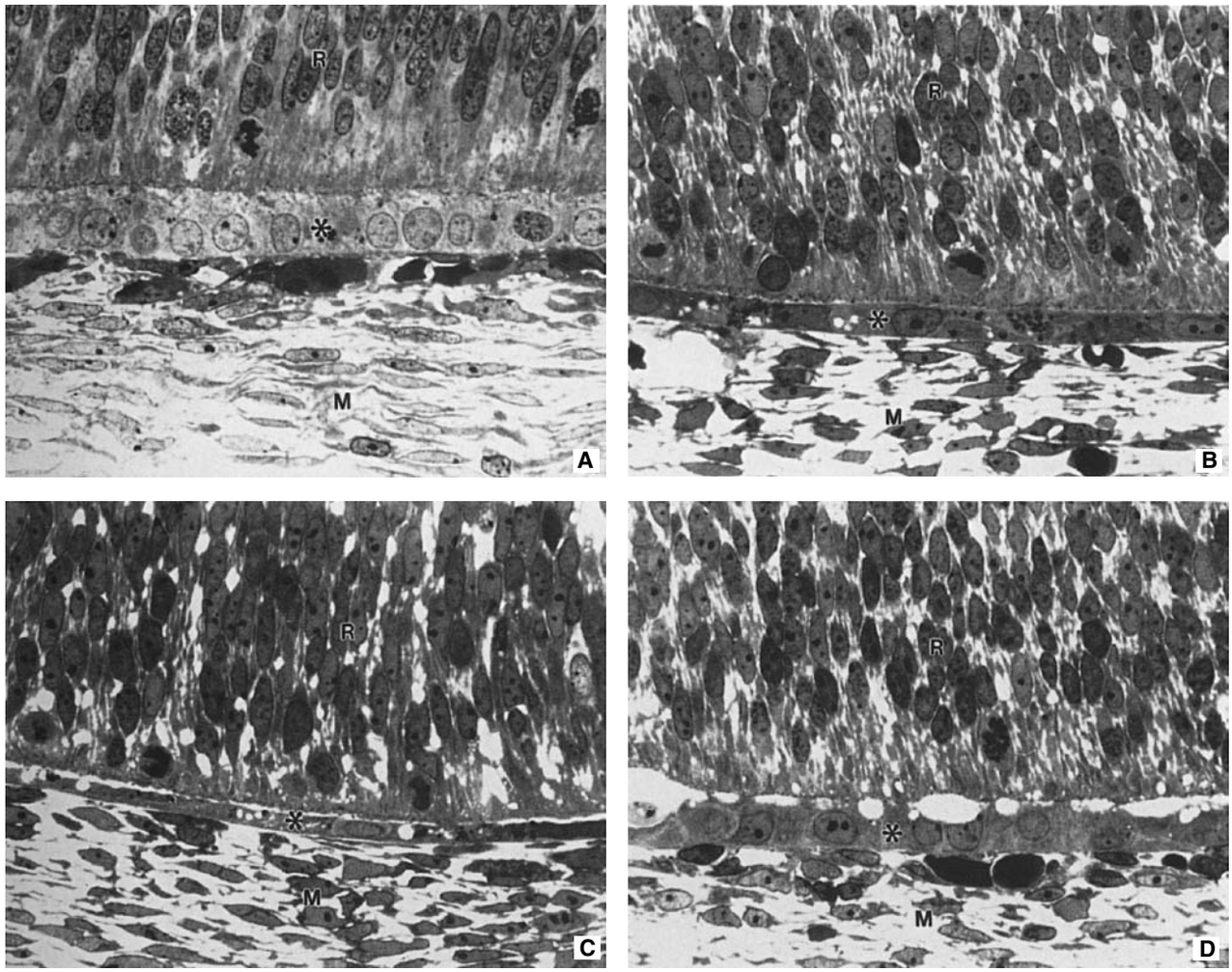

Figure 1.22 Sequential histology of merle ocular dysgenesis (MOD). **A.** Normal canine eye on day 30 of gestation. Note the cuboidal appearance of the nonpigmented retinal pigment epithelium (RPE; ·), which is closely apposed to the neural retina (R). The nuclei closest to the RPE are those of the outer neuroblastic layer. M, periocular mesenchyme—anlage of the choroid and sclera. **B.** MOD-affected eye on day 35 of gestation. The RPE (·) is shortened and contains a few intracytoplasmic vacuoles. **C** and **D.** MOD-affected eye on day 35 of gestation. The RPE (·) has become progressively thinner and exhibits a large number of vacuoles. Separation of the degenerating RPE from the neural retina also can be seen. (Reprinted with permission from Cook, C., Burling, K., & Nelson, E. (1991) Embryogenesis of posterior segment colobomas in the Australian shepherd dog. *Progress in Veterinary & Comparative Ophthalmology*, **1**, 163–170.)

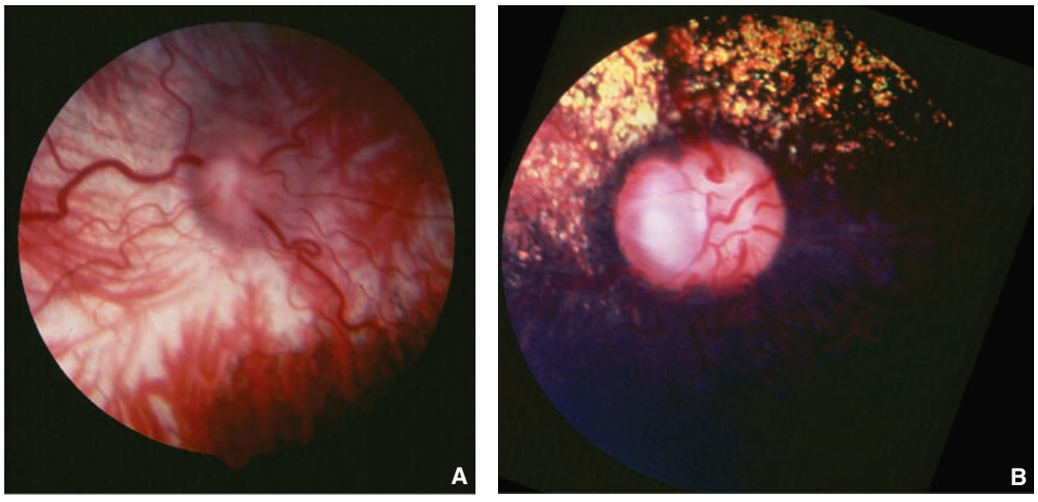

Figure 1.23 **A.** Fundus photograph of choroidal hypoplasia associated with Collie eye anomaly. Note the white sclera with superimposed choroidal and retinal vasculature. **B.** Optic nerve coloboma in a Collie affected with Collie eye anomaly. The coloboma is located temporally adjacent to an area of mild choroidal hypoplasia (identified by absence of tapetum and visible choroidal vasculature).

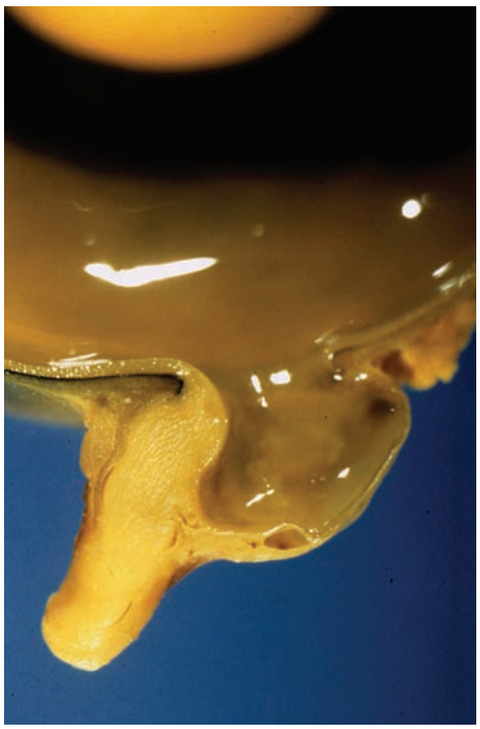

Figure 1.24 Gross photograph of an optic nerve coloboma in a Collie. Note the excavation of thinned sclera lined by glial tissue (neuroectoderm) continuous with retina. (Reprinted with permission from Wilcock, B. (2007) *Pathologic Basis of the Veterinary Disease*, 4th ed. (eds. McGavin, M.D. & Zachary, J.F.). St. Louis, MO: Elsevier.)

Table 1.4 Comparative features of merle ocular dysgenesis and Collie eye anomaly.

	Merle Ocular Dysgenesis	Collie Eye Anomaly
Coat color	Homozygous merle	No correlation
Microphthalmia	Frequent	Rare/mild
Choroidal hypoplasia	Extensive scleral/ retinal defects	Common, localized
Optic nerve coloboma	Rare	Frequent
Cataract	Frequent	Rare
Iris coloboma	Frequent	Rare

Reprinted with permission from Cook, C., Burling, K., & Nelson, E. (1991) Embryogenesis of posterior segment colobomas in the Australian Shepherd dog. *Progress in Veterinary & Comparative Ophthalmology*, **1**, 163–170.

membranes also occur sporadically in other breeds (Strande et al., 1988).

Because most structures of the ocular anterior segment are of neural crest origin, it is tempting in cases of anterior segment anomalies to incriminate this cell population as being abnormal in differentiation, migration, or both. This

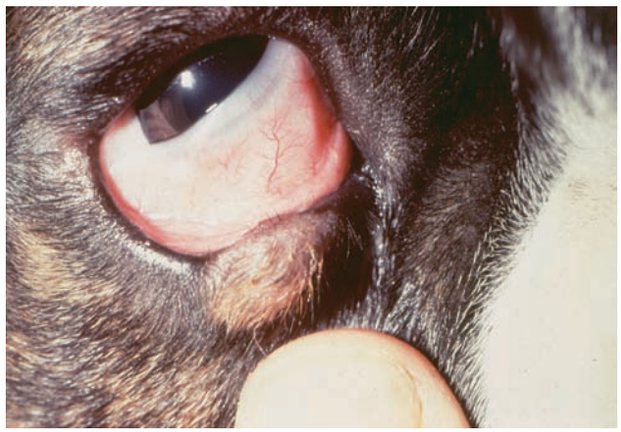

Figure 1.25 Eyelid dermoid in a Boxer dog. The tissue is histologically normal skin in a grossly normal location, but abnormal in configuration, representing a hamartoma. (Courtesy of Robert Peiffer.)

Figure 1.26 Limbal dermoid in a Lhasa Apso puppy. This is an example of a choristoma (histologically normal tissue in an abnormal location).

theory has resulted in labeling these conditions, when they occur in humans, as ocular neurocristopathies, particularly when other anomalies exist in tissues that are largely derived from the neural crest (e.g., craniofacial connective tissue, teeth; Bahn et al., 1984; Kupfer et al., 1975; Kupfer & Kaiser-Kupfer, 1978; Shields et al., 1985; Waring et al., 1975). When considering this theory, it is important to realize two concepts. First, the neural crest is the predominant cell population of the developing craniofacial region, particularly the eye. In fact, the list of ocular tissues *not* derived from neural crest is relatively small (see Table 1.2). Thus, the fact that most malformations of this region involve crest tissues may reflect their ubiquitous distribution rather than their common origin. The normal development of the choroid and sclera (also of neural crest origin) in most of these "neural crest syndromes" argues against a primary neural crest anomaly. Second, the neural crest is an actively migrating

population of cells and can be easily influenced by adjacent cell populations. Thus, the perceived anomaly of neural crest tissue may, in many cases, be a secondary effect.

Much of the maturation of the iridocorneal angle occurs late during gestation and during early postnatal life in the dog, but earlier events may influence development of the anterior segment. Anterior segment dysgenesis syndromes characterized primarily by axial defects in corneal stroma and endothelium, accompanied by corresponding malformations in the anterior lens capsule and epithelium (i.e., Peters' anomaly), most likely represent a manifestation of abnormal keratolenticular separation (Fig. 1.27 and Fig. 1.28). This spectrum of malformations that mimic Peters' anomaly can be induced by teratogen exposure in mice before optic sulcus invagination (Fig. 1.29 and Fig. 1.30; Cook, 1989; Cook & Sulik, 1988; Cook et al., 1987). Similar syndromes of anterior segment dysgenesis have been identified in humans following ethanol exposure (Miller et al., 1984; Stromland et al., 1991).

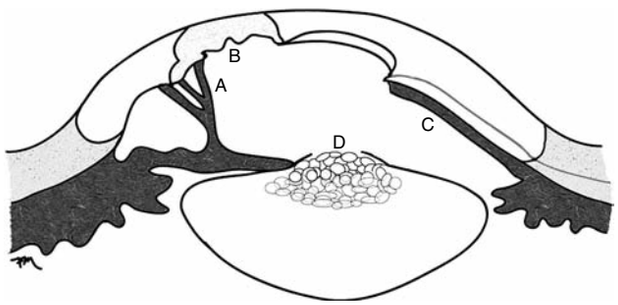

Figure 1.27 Clinical features of Peters' anomaly (anterior segment dysgenesis) resulting from abnormal separation of the lens vesicle from the surface ectoderm. **A.** Persistent pupillary membranes. **B.** Corneal opacity associated with defect in corneal endothelium, Descemet's membrane, and corneal stroma (neural crest). **C.** Iris hypoplasia. **D.** Anterior lenticonus and anterior polar cataract associated with partial defect in anterior lens capsule. (Drawing by Farid Mogannam.)

The size of the lens vesicle is determined by the area of contact between the optic vesicle and the surface ectoderm. Thus, factors influencing the size of the optic vesicle or the angle at which the optic vesicle approaches the surface ectoderm may affect the ultimate size of the lens vesicle. Microphakia resulting from optic vesicle deficiencies may be initiated very early in gestation (i.e., during formation of the neural plate). Microphakia associated with lens luxation has been described in two unrelated Siamese kittens (Molleda et al., 1995); as the globes were apparently otherwise normal, a primary abnormality in the lens placode ectoderm can be postulated. Aphakia is much more rare, and may occur through failure of contact between the optic vesicle and the surface ectoderm during the period when the surface ectoderm can respond to its inductive influences. As the anterior lens epithelium is required for induction of the corneal endothelium, this early initiation of aphakia would be associated with dysgenesis of the cornea and (likely) anterior uvea. Alternatively, normal induction of a lens vesicle followed by later involution would be expected to result in an eye with more normal anterior segment morphology. The lens aplasia (lap) mouse demonstrates faulty lens basement membrane formation associated with apoptosis and involution of the rudimentary lens vesicle (Aso et al., 1995, 1998). Sporadic cases of aphakia have been described in domestic animals, including a cat with associated retinal detachment but apparently normal iridocorneal structures (histopathology not available; Peiffer, 1982), and a litter of Saint Bernard puppies with multiple ocular malformations (Martin & Leipold, 1974). In humans, *in utero* exposure to rubella or parvovirus B can result in aphakia; anterior segment structures are variably affected (Hartwig et al., 1988). Abnormalities in lens shape (e.g., spherophakia, lens coloboma) may actually represent a primary abnormality in the ciliary processes, zonular fibers, or both, resulting in a lack of tension on the lens (Fig. 1.31 and Fig. 1.32). Thus, the term *coloboma* may be inaccurate when used in reference to a flattened equatorial portion of the lens that is not a true lens defect.

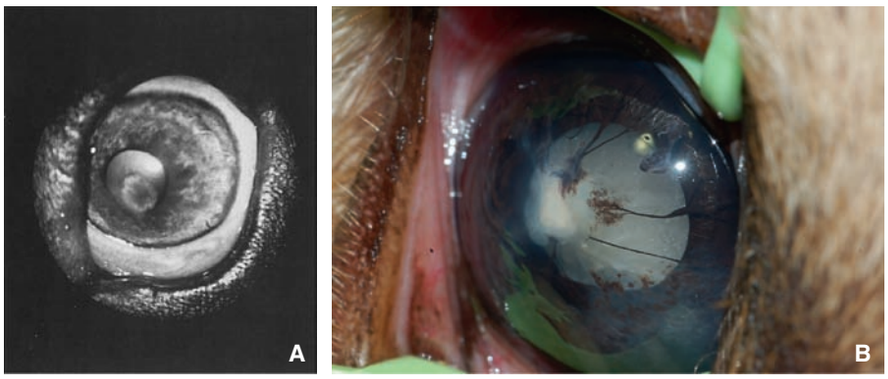

Figure 1.28 **A.** Clinical photograph of a puppy with Peters' anomaly exhibiting microphthalmia, a central corneal opacity, anterior axial cataract, and persistent pupillary membranes. **B.** A more severe form of anterior segment dysgenesis with visible lens material trapped within the axial cornea, accompanied by persistent pupillary membranes leading to the corneal defect.

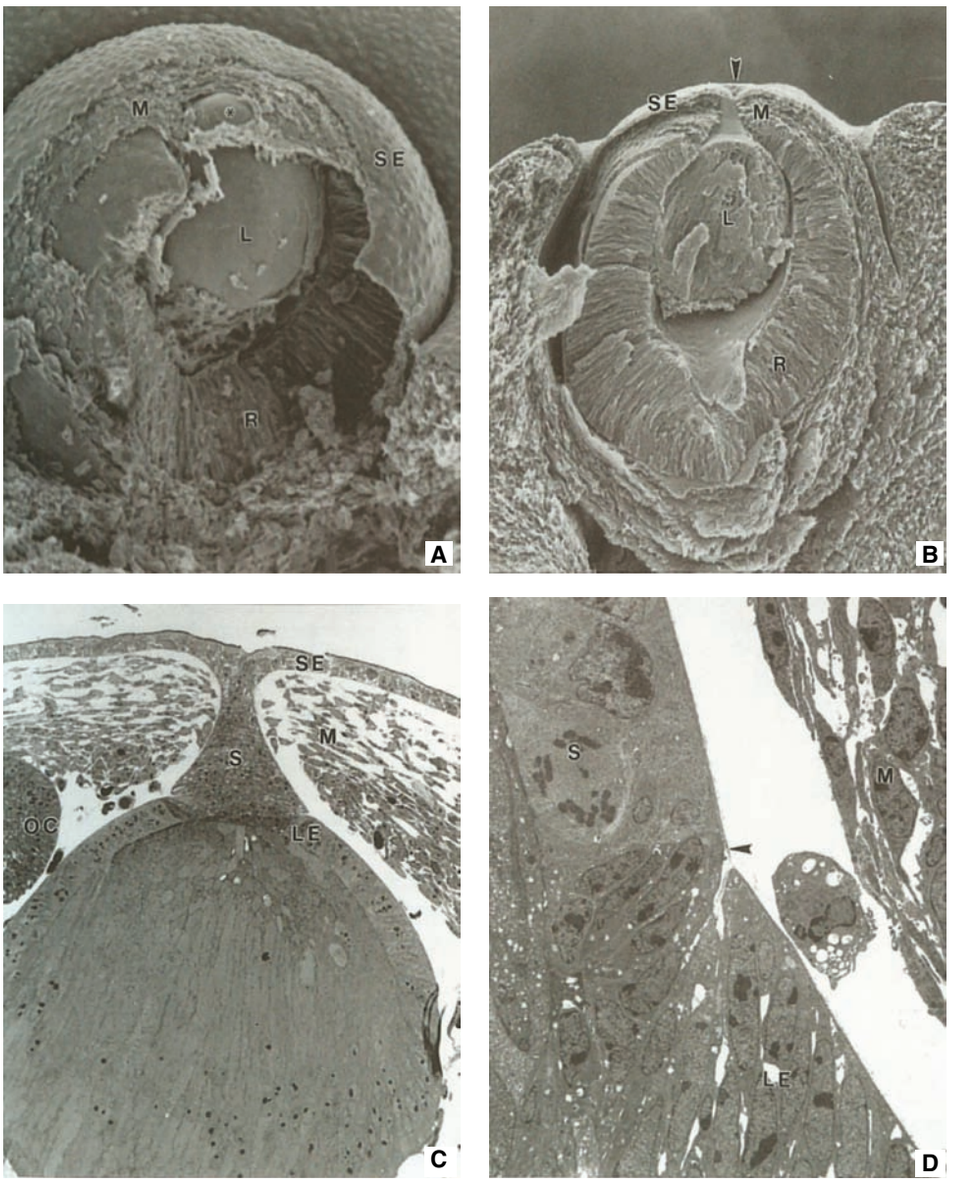

Figure 1.29 Keratolenticular dysgenesis induced by teratogen exposure in mice. **A.** Mouse embryo following acute exposure to ethanol during gastrulation. Delay in separation of the lens vesicle (L) from the surface ectoderm (SE) results in an anterior lenticonus (*) and failure of the mesenchyme (M) to complete its axial migration to form the corneal stroma, endothelium, and iris stroma. R, retinal primordium. Original magnification, 166×. **B**, **C**, and **D.** Mouse embryo following acute exposure to 13-*cis*-retinoic acid during gastrulation. A large keratolenticular stalk (S) persists and is continuous axially with the SE. The arrow in **B** indicates the incompletely closed lens pore. **D** is a transmission electron microscopic view of the stalk seen in **C.** There is discontinuity between the lens epithelium (LE) and the stalk epithelium (S). Adjacent neural crest mesenchyme (M) is visible, and two layers of basement membrane can be seen in **D**, bridging the lens–stalk junction as well as dividing the two zones. Mechanical interference with the axial migration of neural crest cells is responsible in this model for malformations, which mimics Peters' anomaly in the human. OC, optic cup. (Reprinted with permission from Cook, C. (1995) Embryogenesis of congenital eye malformations. *Veterinary and Comparative Ophthalmology*, **5**, 109–123.)

Uveal Cysts

Uveal cysts occur through failure of adhesion of the inner and outer layers of the optic cup. In the dog, they are most commonly identified as single or multiple spherical pigmented masses within the pupil or free-floating within the anterior chamber (Fig. 1.33 and Fig. 1.34). They appear to have a genetic predilection. In the cat, they are more often thick-walled and remain attached to the posterior iris surface, causing anterior displacement of the iris and shallowing of the anterior chamber, and may result in secondary glaucoma (Gemensky-Metzler et al., 2004). In cats they also

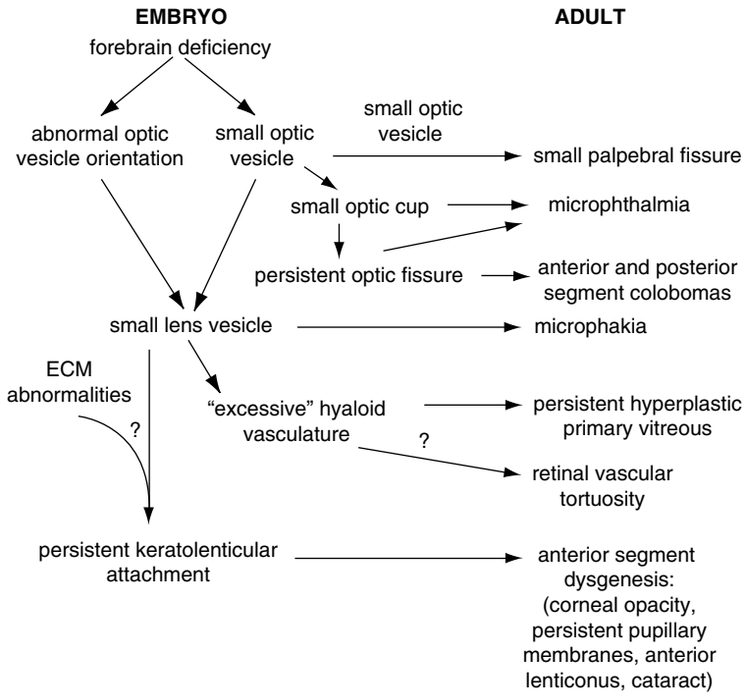

Figure 1.30 The relationship between microphthalmia and associated ocular malformations. An early embryonic insult (during gastrulation) leads to a deficiency in the forebrain and its derivatives, the optic sulci. The subsequently small optic vesicle often exhibits an abnormal relationship to the surface ectoderm, which is programmed (by the underlying neural crest) to form the lens. The result is a spectrum of malformations in the adult, including microphthalmia, microphakia, colobomas, persistent hyperplastic primary vitreous, and anterior segment dysgenesis. ECM, extracellular matrix. (Reprinted with permission from Cook, C. (1995) Embryogenesis of congenital eye malformations. *Veterinary and Comparative Ophthalmology*, **5**, 109–123.)

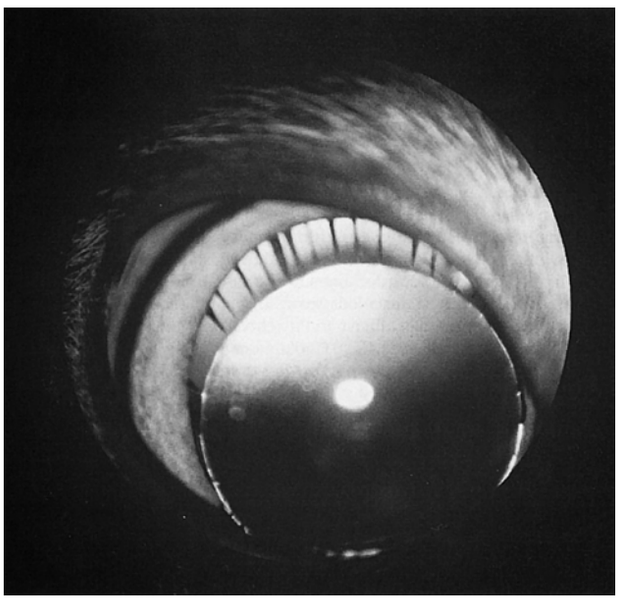

Figure 1.31 Microphakia and spherophakia in a cat. Note the elongated ciliary processes. The globe was not microphthalmic, and this most likely represented a primary abnormality in the surface ectoderm destined to become lens placode.

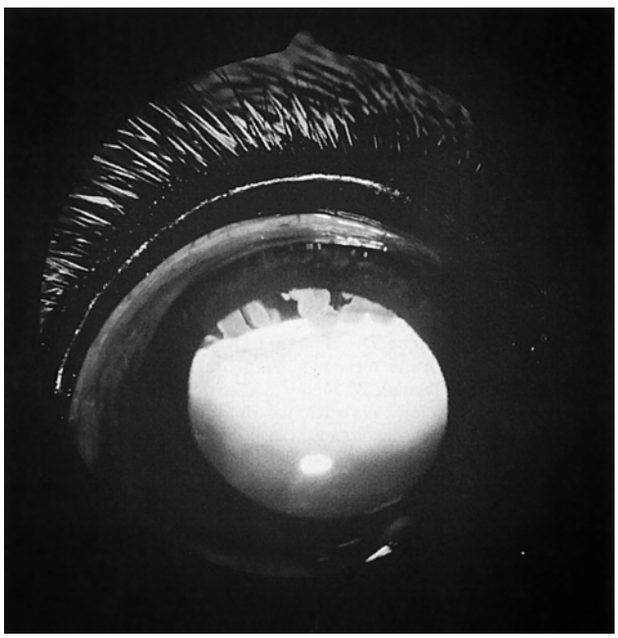

Figure 1.32 Nonpigmented ciliary body cysts in a cat. Note the flattened lens equator, which would incorrectly be called a lens coloboma. In this case, a medulloepithelioma of the ciliary body resulted both in the cysts and in the localized absence of zonules. Failure of normal traction by the zonule on the lens equator resulted in this flattened appearance. (Courtesy of Kristina Burling.)

appear to have a genetic predisposition, with Burmese cats overrepresented (Blacklock et al., 2016). When uveal cysts originate within the ciliary body, they can be nonpigmented (see Fig. 1.32).

Uveal cysts are often seen associated with pigmentary uveitis or pigmentary and cystic glaucoma in Golden Retriever dogs and other breeds. There has been a great deal of speculation about whether the cysts may play a causal role in the inflammatory disease process (Pumphrey et al., 2013; Townsend & Gornik, 2013). Uveal cysts seen in dogs affected

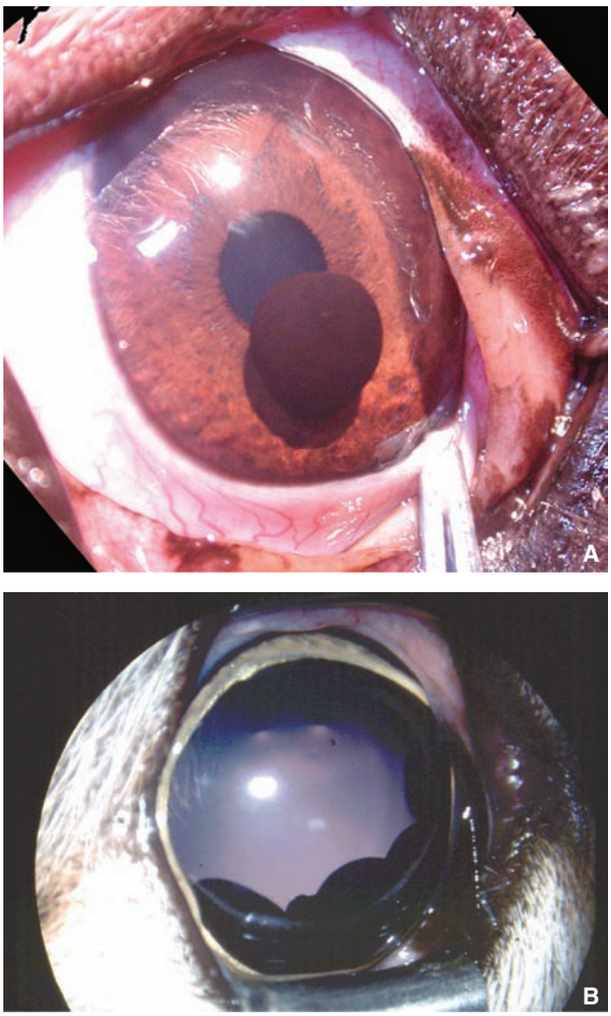

Figure 1.33 Iris cysts. **A.** Single iris cyst in a dog. **B.** Multiple iris cysts in a cat. In cats, these cysts are often thick-walled and remain attached to the posterior iris surface, causing anterior displacement of the iris and a shallow anterior chamber.

Figure 1.34 Histologic appearance of a uveal cyst on the posterior iris surface. These cysts form beneath the posterior pigmented epithelium and frequently separate to become free-floating spheres within the anterior chamber. (Courtesy of Robert Peiffer.)

with uveitis have a unique clinical appearance, being more translucent, irregularly shaped, and often adherent to the lens or cornea. This is in distinct contrast to the cysts commonly seen in other canine breeds with complete lack of inflammation.

Congenital Ocular Anomalies in Horses

A syndrome of multiple congenital ocular anomalies (MCOA) has been identified as a bilaterally symmetrical, inherited condition in several breeds of horses, most notably the Rocky Mountain breed, silver mutant ponies, and miniature horses (Andersson et al., 2011; Komaromy et al., 2011; Plummer & Ramsey, 2011; Ramsey et al., 1999a, 1999b; Fig. 1.35). Affected individuals most often have a silver coat color, and correlation with the Silver Dapple locus is suspected. The condition in the heterozygote is characterized by cysts of the posterior iris, ciliary body, and peripheral retina, indicating failure of adhesion of the inner and outer layers of the optic cup. These cysts are consistently located temporally, not associated with the optic fissure. Areas of current or previous retinal detachment were further manifestations of abnormal cup invagination and adhesion. The spectrum of anterior segment malformations seen in homozygous individuals included megalocornea, deep anterior chamber, iris hypoplasia, and cataract. Increased thickness of the central and peripheral corneas was noted and increased with age. Intraocular pressures were normal (Ramsey et al., 1999b). The syndrome in Rocky Mountain horses appears to exhibit codominant inheritance (Ewart et al., 2000). Cataracts have been identified in Exmoor ponies, with a suspected sex-linked mode of inheritance (Pinard & Basrur, 2011). Other congenital anomalies appear to occur rarely in horses, with occasional neonatal diagnosis of retinal and conjunctival hemorrhages thought to be due to injury during parturition (Barsotti et al., 2013).

Congenital Cataracts

Congenital cataracts resulting from abnormal formation of primary or secondary lens fibers would be expected to be localized to the nuclear region, and be nonprogressive. However, an early effect on the primary lens fibers may extend to involve the secondary fibers, resulting in a congenital cataract that progresses to involve the entire lens.

Abnormal lens vesicle invagination, separation, or defects in the lens epithelium or capsule would result in a cataract (with or without anterior or posterior lenticonus; Ori et al., 2000) that would remain associated with the peripheral portion of the lens, with the secondary lens fibers forming underneath (e.g., Old English Sheepdog, Barrie et al., 1979; Cavalier King Charles Spaniel, Narfstrom & Dubielzig, 1984). Congenital cataracts associated with mild microphthalmia (Miniature Schnauzer, Gelatt et al., 1983; Monaco

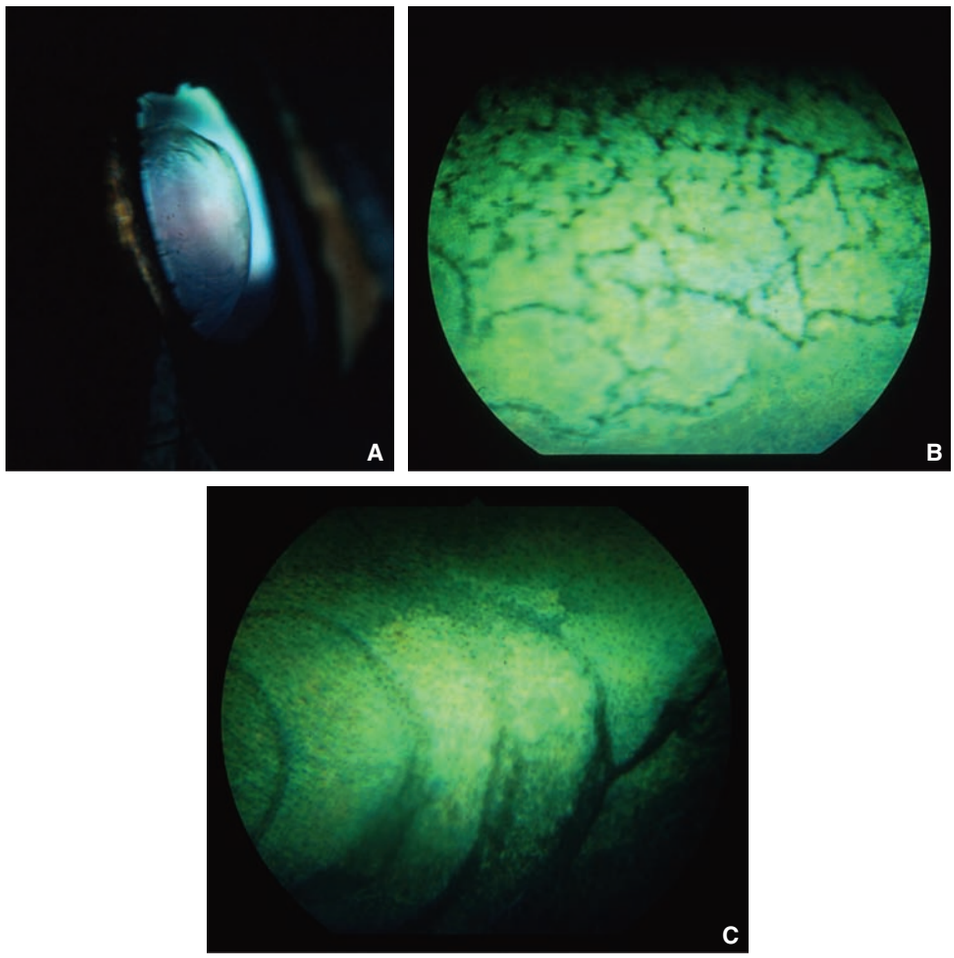

Figure 1.35 Spectrum of ocular lesions seen in Rocky Mountain horses. **A.** A large translucent cyst arising from the lateral part of the ciliary body extends into the vitreous cavity and occupies part of the temporal pupillary axis of the right eye. **B.** Retinal dysplasia is characterized by numerous pigmented folds located in the superior peripapillary neurosensory retina. **C.** Multiple, well-delineated, darkly pigmented curvilinear streaks of retinal pigment epithelium are present in the peripheral right tapetal fundus. These streaks originate and terminate at the ora ciliaris retinae and extend toward the optic papilla. They represent demarcation lines from previous retinal detachments and are referred to clinically as "high-water markers." (Reprinted with permission from Ramsey, D.T., Ewart, S.L., Render, J.A., et al. (1999) Congenital ocular abnormalities of Rocky Mountain horses. *Veterinary Ophthalmology*, **2**, 47–59.)

et al., 1985; Samuelson et al., 1987) may result from early abnormalities in the lens placode/epithelium, and they may involve the lens nucleus, cortex, or both. In the Miniature Schnauzer, these lesions are recessively inherited, typically bilateral, and initially involve the posterior subcapsular region with rapid progression (Gelatt et al., 1983; Zhang et al., 1991).

Congenital Glaucoma

Malformations of the iridocorneal angle (i.e., goniodysgenesis) have been described in several breeds, including the Basset Hound (Martin & Wyman, 1968; Wyman & Ketring, 1976) and the Bouvier des Flandres (van Rensburg et al., 1992). The iridocorneal angles of affected animals are malformed at birth, but the IOP often remains normal until middle age. Thus, the relationship between angle conformation and glaucoma is unclear. In English Springer Spaniels, a correlation was observed between pectinate ligament dysplasia and glaucoma (Bjerkas et al., 2002). Although pectinate ligament dysplasia is a congenital malformation, it may appear to clinically progress over time, as assessed by sequential gonioscopic evaluations in Flat-Coated Retrievers (Pearl et al., 2015).

Goniodysgenesis is characterized by abnormal tissue bridging the ciliary cleft. During normal development, this sheet undergoes rarefaction to form the pectinate ligament during the first three postnatal weeks (Martin, 1974; Samuelson & Gelatt, 1984a). Failure of this membrane to undergo normal atrophy is thought to result in goniodysgenesis. Congenital

glaucoma associated with presumed primary iridoschisis (i.e., degeneration of the anterior iris) has been described in a cat (Brown et al., 1994).

Persistent Hyperplastic Primary Vitreous/ Persistent Hyperplastic Tunica Vasculosa Lentis

Variable persistence of the hyaloid occurs in association with many other types of malformations, including microphthalmia, microphakia, cataract, and retinal dysplasia (Fig. 1.36; Bayon et al., 2001; Boeve et al., 1992). Persistent hyperplastic primary vitreous/persistent hyperplastic tunica vasculosa lentis (PHPV/PHTVL) may occur secondary to other malformations or as a primary, spontaneous failure of vascular regression. This condition has been described as an inherited trait in the Doberman (Stades, 1980; van der Linde-Sipman et al., 1983) and the Bouvier des Flandres (van Rensburg et al., 1992), and has been identified in two cats (Allgoewer & Pfefferkorn, 2001). In the Doberman, the genetics appear to be something more than simple recessive (Stades, 1983).

The mechanism involved is failure of normal vascular regression and hyperplasia of the persistent tissue. Normal vitreous may have antiangiogenic properties, and it may be essential for initiating regression of the hyaloid. Expression of the Arf tumor suppressor gene in perivascular cells may repress VEGF expression, thus promoting hyaloid regression in mice (Martin et al. 2004). Thus, the primary abnormality in PHPV/PHTVL may rest with the product of the ciliary epithelium (i.e., secondary vitreous).

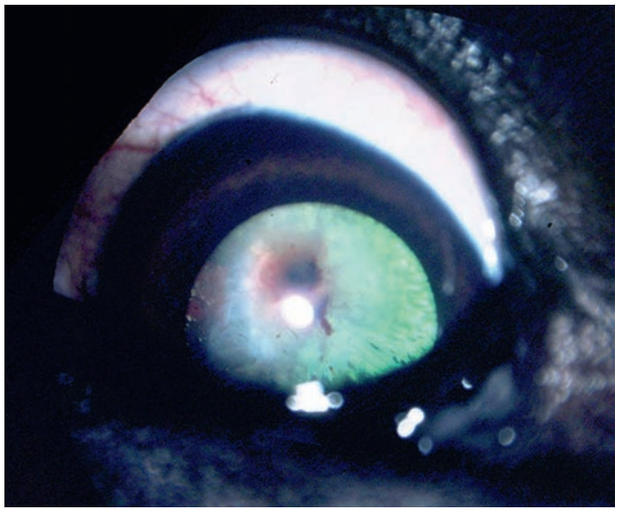

Figure 1.36 Persistent hyperplastic primary vitreous in a puppy associated with a posterior subcapsular cataract. This eye is also microphthalmic.

Retinal Dysplasia

Abnormal retinal differentiation results in rosettes and multifocal disorganization known as retinal dysplasia. Retinal folds without rosette formation may result from inequity in the relative growth rates of the inner (i.e., retinal) and outer (i.e., RPE) layers of the optic cup (Fig. 1.37 and Fig. 1.38). This is a particularly likely pathogenesis in cases in which the folds resolve as the animal matures; this is seen most commonly among Collies. These folds do not represent abnormal differentiation and thus are not

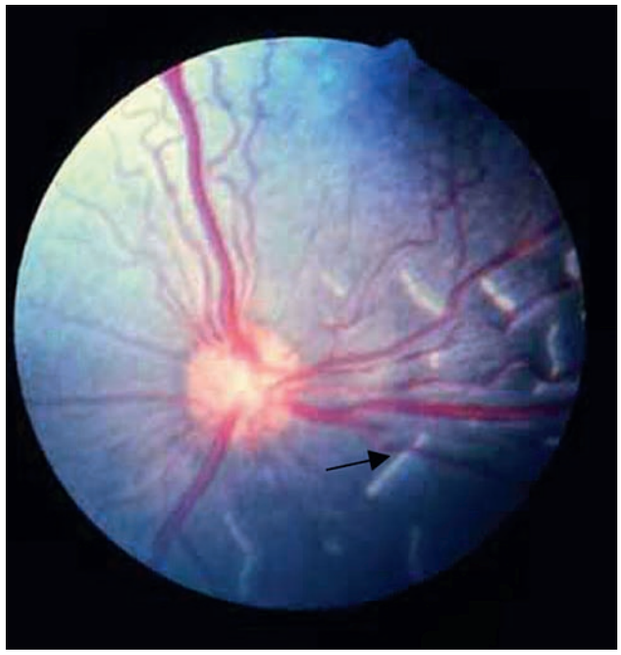

Figure 1.37 Fundus photograph of retinal folds in a young American Cocker Spaniel. These appear as single or multiple white curvilinear streaks. Elevation of a retinal vessel crossing a fold (arrow) can be seen.

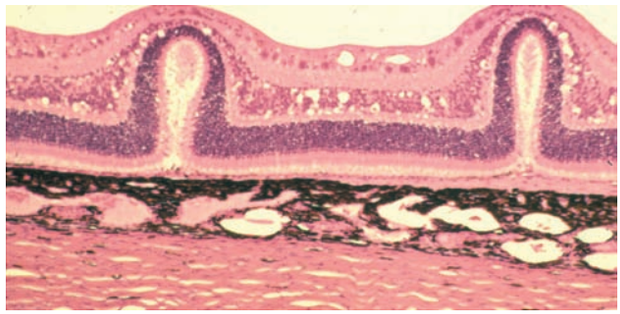

Figure 1.38 Histologic appearance of retinal folds. Note the normal stratification of the retinal layers and the mechanical distortion caused by disparate growth of the neural retina (inner optic cup) and the underlying RPE (outer optic cup). (Courtesy of Robert Peiffer.)

accurately referred to as dysplasia. Simple folding in the retina has been described in the American Cocker Spaniel (MacMillan & Lipton, 1978) and the Beagle (Heywood & Wells, 1970; Schiavo & Field, 1974). The genetic relationship between simple folds and true retinal dysplasia is undetermined.

True retinal dysplasia is characterized by disorganized development, the hallmark of which is the rosette. Abnormal or incomplete contact between the inner and outer layers of the optic cup during embryogenesis can result in dysplasia, with the most severe form associated with complete retinal nonattachment. This usually occurs in eyes that are microphthalmic with multiple ocular anomalies (e.g., Bedlington terrier, Rubin, 1963, 1968; Sealyham terrier, Ashton et al., 1968; and American Pit Bull terrier, Rodarte-Almeida et al., 2016). In the Labrador Retriever, retinal dysplasia genetically associated with skeletal anomalies is inherited as an autosomal dominant trait (Barnett et al., 1970; Carrig et al., 1988; Nelson & Macmillan, 1983). A similar form of inherited skeletal-ocular dysplasia is seen in the Samoyed dog (Aroch et al., 1996; Meyers et al., 1983).

Multifocal retinal rosettes in a retina that is partially attached to the underlying RPE represent the most common form of retinal dysplasia (Fig. 1.39 and Fig. 1.40). This condition has been described extensively in the English Springer Spaniel (Lavach et al., 1978; O'Toole et al., 1983). Retinal dysplasia occurs sporadically in other breeds (Bedford, 1982b) and species (Murphy et al., 1985). Multifocal, "geographic" retinal dysplasia most likely represents a later initiation of retinal disorganization. The dysplastic changes are first apparent at 45–50 days of gestation. Focal loss of cell junctions of the external limiting membrane is seen, with proliferation of neuroblasts in the retina forming rosettes (Whiteley, 1991). Retinal differentiation and maturation in the dog continue during the first 40 days postnatal. In addition, maturation of the tapetum during the first 6 months results in an inconsistent ability to detect mild forms of retinal dysplasia in puppies less than 10 weeks of age (Holle et al., 1999).

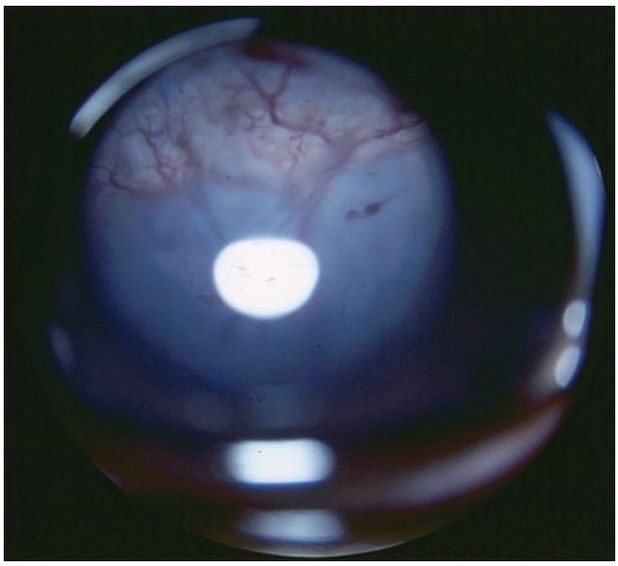

Figure 1.39 Geographic retinal dysplasia in an English Springer Spaniel. The retina is detached and lies just posterior to the lens; there are many folds visible.

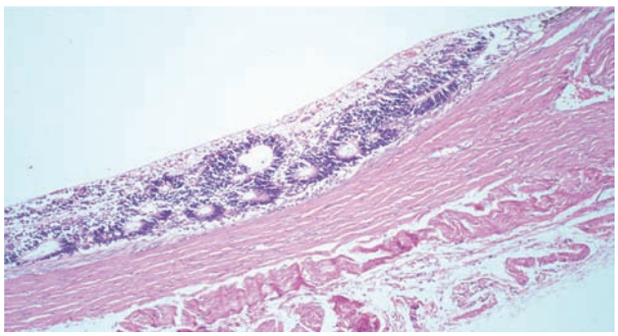

Figure 1.40 Histologic appearance of geographic retinal dysplasia. The retina exhibits disorganization and classic rosette formation. Note also the hypoplastic choroid. (Courtesy of Robert Peiffer.)

An unusual form of RPE dysplasia with duplication of neural retina in the outer layer of the optic cup has been described in several mutant mouse strains (Bumsted & Barnstable, 2000; Cook et al., 1991b). Large colobomas of the choroid and sclera in the areas adjacent to the dysplastic RPE illustrate the importance of this layer in coordinating differentiation of the neural crest.

Viral-induced "retinal dysplasia" has been associated with early postnatal exposure to canine herpesvirus and prenatal exposure to bovine viral diarrhea virus (Bistner et al., 1970; Brown et al., 1975; Kahrs et al., 1970), bluetongue virus in lambs (Silverstein & Al, 1971), and feline panleukopenia virus (Percy et al., 1975). Histopathologically, affected retinas are characterized by early inflammatory cell infiltrate and, later, by necrosis, gliosis, and diffuse disorganization of cell layers. Similar postnatal retinal disorganization can be induced in the dog by radiation exposure (Shively et al., 1970, 1972). These conditions are more accurately classified as teratogen-induced necrosis and degeneration rather than as dysplasia.

Optic Nerve Hypoplasia

Though difficult to document experimentally, optic nerve hypoplasia most likely results from a primary abnormality in the number or ultimate differentiation of the retinal ganglion cells (Fig. 1.41). Hypovitaminosis A in cattle can result

Figure 1.41 Optic nerve hypoplasia in an 8-week-old Alsatian puppy. This was a unilateral lesion and the pup presented with anisocoria. (Courtesy of Robert Peiffer.)

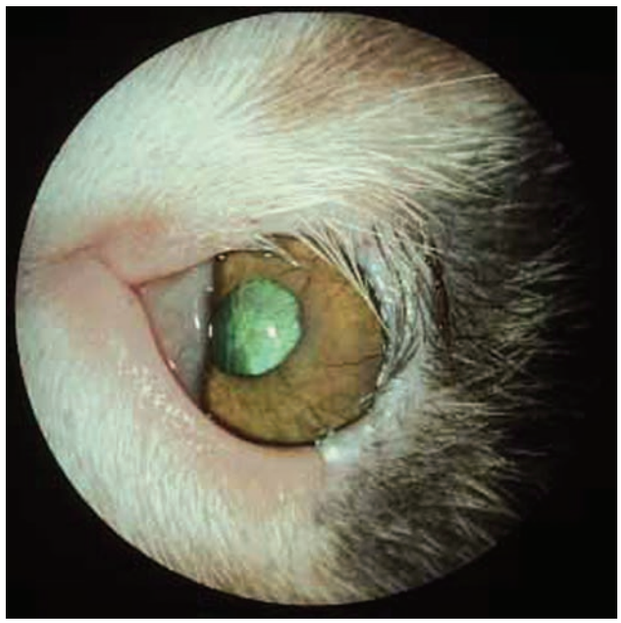

Figure 1.42 Eyelid coloboma in a kitten. The eyelid margin is absent from the temporal two-thirds of the upper lid. There is keratitis due to exposure and trichiasis. The eye also exhibits microphthalmia, dyscoria, and persistent pupillary membranes.

in stenosis of the optic foramen with secondary optic nerve degeneration, incorrectly labeled hypoplasia. Colobomas of the optic nerve result from failure of the optic fissure to close, as described for "typical" colobomas. Myelination of the optic nerve progresses from the brain to the eye during the first 3 weeks postnatal (Fox, 1963). Reduction in the amount of myelinization leads to a small optic disc that can mimic hypoplasia but is unassociated with vision deficits (termed micropapilla).

Eyelid Coloboma

The eyelids and palpebral fissure are initially induced at the time of contact of the optic vesicle with the surface ectoderm. This is also the time of induction of the lens placode. Eyelid agenesis (coloboma) occurs in domestic cats, often with concurrent persistent pupillary membranes, keratolenticular dysgenesis, and subtle to severe microphthalmia (Fig. 1.42; Glaze, 2005; Koch, 1979; Martin et al., 1997; Narfstrom, 1999). Eyelid colobomas occur less commonly in dogs (Fig. 1.43) and a case of upper eyelid agenesis has also been described in a Peregrine Falcon (Aguirre et al., 1972; Murphy et al., 1985) and in two sibling snow leopards (Hamoudi et al., 2013). The snow leopards also exhibited microphthalmia, typical anterior segment dysgenesis, and persistent hyaloid.

The receptivity of the surface ectoderm to the inductive influences of the optic vesicle is highly spatiotemporally

Figure 1.43 A Cavalier King Charles Spaniel with bilateral lower eyelid colobomas and dermoids. Note the notch defects in the central portion of the lower lids and the abnormal hair growth adjacent to the defects.

specific. The fairly consistent location of the defect in the temporal upper eyelid leads to suspicion of an abnormal orientation of the optic vesicle as it approaches the surface ectoderm, possibly eccentrically contacting the surface ectoderm in an area that is only partially receptive.

References

Adams, S.B., Horstman, L., & Hoerr, F.J. (1983) Periocular dermoid cyst in a calf. *Journal of the American Veterinary Medical Association*, **182**, 1255–6.

Aguirre, G., Rubin, L., & Bistner, S. (1972) Development of the canine eye. *American Journal of Veterinary Research*, **33**, 2399.

Akiya, S., Uemura, Y., Tsuchiya, S., et al. (1986) Electron microscopic study of the developing human vitreous collagen fibrils. *Ophthalmic Research*, **18**, 199–202.

Allen, L., Burian, H., & Braley, A. (1955) A new concept of the development of the anterior chamber angle: Its relationship to developmental glaucoma and other structural anomalies. *Archives of Ophthalmology*, **53**, 783–798.

Allgoewer, I. & Pfefferkorn, B. (2001) Persistent hyperplastic tunica vasculosa lentis and persistent hyperplastic primary vitreous (PHTVL/PHPV) in two cats. *Veterinary Ophthalmology* **4**, 161–164.

Anderson, D. (1981) The development of the trabecular meshwork and its abnormality in primary infantile glaucoma. *Transactions of the American Ophthalmology Society*, **79**, 458–485.

Andersson, L.S., Lyberg, K., Cothran, G., et al. (2011) Targeted analysis of four breeds narrows equine multiple congenital ocular anomalies locus to 208 kilobases. *Mammalian Genome*, **22**, 353–360.

Arnbjerg, J. & Jensen, O. (1982) Spontaneous microphthalmia in two Doberman puppies with anterior chamber cleavage syndrome. *Journal of the American Animal Hospital Association*, **18**, 481–484.

Aroch, I., Ofri, R., & Aizenberg, I. (1996) Haematological, ocular and skeletal abnormalities in a Samoyed family. *Journal of Small Animal Practice*, **37**, 333–339.

Ashton, N. (1966) Oxygen and the growth and development of retinal vessels. *American Journal of Ophthalmology*, **62**, 412–435.

Ashton, N., Barnett, K., & Sachs, D. (1968) Retinal dysplasia in the Sealyham terrier. *Journal of Pathology and Bacteriology*, **96**, 269–272.

Aso, S., Horiwaki, S., & Noda, S. (1995) Lens aplasia: A new mutation producing lens abnormality in the mouse. *Laboratory Animal Science*, **45**, 41–46.

Aso, S., Tashiro, M., Baba, R., et al. (1998) Apoptosis in the lens anlage of the heritable lens aplastic mouse (lap mouse). *Teratology*, **58**, 44–53.

Bahn, C.F., Falls, H.F., Varley, G.A., et al. (1984) Classification of corneal endothelial disorders based on neural crest origin. *Ophthalmology*, **91**, 558–563.

Bard, J., Hay, E., & Meller, S. (1975) Formation of the endothelium of the avian cornea: A study of cell movement *in vivo*. *Developmental Biology*, **42**, 334.

Barishak, Y. (1978) The development of the angle of the anterior chamber in vertebrate eyes. *Documenta Ophthalmologica*, **45**, 329–360.

Barkyoumb, S. & Leipold, H. (1984) Nature and cause of bilateral ocular dermoids in Hereford cattle. *Veterinary Pathology*, **21**, 316–324.

Barnett, K. (1979) Collie eye anomaly. *Journal of Small Animal Practice*, **20**, 537–542.

Barnett, K., Bjorck, G., & Kock, E. (1970) Hereditary retinal dysplasia in the Labrador Retriever in England and Sweden. *Journal of Small Animal Practice*, **10**, 755–759.

Barnett, K.C. & Stades, F.C. (1979) Collie eye anomaly in the Shetland Sheepdog in the Netherlands. *Journal of Small Animal Practice*, **20**, 321–329.

Barrie, K., Peiffer, R., Gelatt, K., et al. (1979) Posterior lenticonus, microphthalmia, congenital cataracts and retinal folds in an Old English Sheepdog. *Journal of the American Animal Hospital Association*, **15**, 715–717.

Barsotti, G., Sgorbini, M., Marmorini, P., & Corazza, M. (2013) Ocular abnormalities in healthy Standardbred foals. *Veterinary Ophthalmology* **16**, 245–250.

Bayon, A., Tovar, M.C., Fernandez Del Palacio, M.J., et al. (2001) Ocular complications of persistent hyperplastic primary vitreous in three dogs. *Veterinary Ophthalmology*, **4**, 35–40.

Bedford, P.G. (1982a) Collie eye anomaly in the Border Collie. *Veterinary Record*, **111**, 34–35.

Bedford, P.G. (1982b) Multifocal retinal dysplasia in the Rottweiler. *Veterinary Record*, **111**, 304–305.

Bedford, P.G. (1998) Collie eye anomaly in the Lancashire Heeler. *Veterinary Record*, **143**, 354–356.

Beebe, D. (1985) Ocular growth and differentiation factors. In: *Growth and Maturation Factors* (ed. Guroff, G.), Vol. **3**, pp. 39–76. New York: Wiley.

Beebe, D.C. & Coats, J.M. (2000) The lens organizes the anterior segment: Specification of neural crest cell differentiation in the avian eye. *Developmental Biology*, **220**, 424–431.

Beebe, D.C., Compart, P.J., Johnson, M.C., et al. (1982) The mechanism of cell elongation during lens fiber cell differentiation. *Developmental Biology*, **92**, 54–59.

Beebe, D.C., Latker, C.H., Jebens, H.A., et al. (1986) Transport and steady-state concentration of plasma proteins in the vitreous humor of the chicken embryo: Implications for the mechanism of eye growth during early development. *Developmental Biology*, **114**, 361–368.

Bellhorn, R.W. (1974) A survey of ocular findings in eight- to ten-month-old Beagles. *Journal of the American Veterinary Medical Association*, **164**, 1114–1116.

Bergsjo, T., Arnesen, K., Heim, P., et al. (1984) Congenital blindness with ocular developmental anomalies, including retinal dysplasia, in Doberman Pinscher dogs. *Journal of the American Veterinary Medical Association*, **184**, 1383–1386.

Berman, M. & Pierro, L. (1969) Lens detachment and choroid fissure closure in the embryonic mouse eye. *American Zoologist*, **9**, 365.

Bertram, T., Coignoul, F., & Cheville, N. (1984) Ocular dysgenesis in Australian Shepherd dogs. *Journal of the American Animal Hospital Association*, **20**, 177.

Binns, W., Thacker, E.J., James, L.F., et al. (1959) A congenital cyclopian-like malformation in lambs. *Journal of the American Veterinary Medical Association*, **134**, 180–183.

Bistner, S., Rubin, L., & Roberts, S. (1971) A review of persistent pupillary membranes in the Basenji dog. *Journal of the American Animal Hospital Association*, **7**, 143–157.

Bistner, S., Rubin, L., & Saunders, L. (1970) The ocular lesions of bovine viral diarrhea-mucosal disease. *Veterinary Pathology*, **7**, 275.

Bjerkas, E., Ekesten, B., & Farstad, W. (2002) Pectinate ligament dysplasia and narrowing of the iridocorneal angle associated with glaucoma in the English Springer Spaniel. *Veterinary Ophthalmology*, **5**, 49–54.

Blacklock, B. T., Grundon, R.A., Meehan, M., et al. (2016) Uveal cysts in domestic cats: A retrospective evaluation of thirty-six cases. *Veterinary Ophthalmology*, **19**, 56–60.

Blackwell, R. & Cobb, E. (1959) A hydrocephalus lethal in Hereford cattle. *Journal of Heredity*, **50**, 143–147.

Boeve, M.H., Stades, F.C., Linde-Sipman, J.S.V.D., et al. (1992) Persistent hyperplastic tunica vasculosa lentis and primary vitreous (PHTVL/PHPV) in the dog: A comparative review. *Progress in Veterinary & Comparative Ophthalmology*, **2**, 163.

Boroffka, S.A., Verbruggen, A.M., Boeve, M.H., et al. (1998) Ultra-sonographic diagnosis of persistent hyperplastic tunica vasculosa lentis/persistent hyperplastic primary vitreous in two dogs. *Veterinary Radiology and Ultrasound*, **39**, 440–444.

Bremer, F.M. & Rasquin, F. (1998) Histochemical localization of hyaluronic acid in vitreous during embryonic development. *Investigative Ophthalmology & Visual Science*, **39**, 2466–2469.

Bressan, G.M., Daga-Gordini, D., Colombatti, A., et al. (1993) Emilin, a component of elastic fibers preferentially located at the elastin–microfibrils interface. *Journal of Cell Biology*, **121**, 201–212.

Briziarelli, G. & Abrutyn, D. (1975) Atypical coloboma in the optic disc of a Beagle. *Journal of Comparative Pathology*, **85**, 237–240.

Brown, A., Munger, R., & Peiffer, R. (1994) Congenital glaucoma and iridoschisis in a Siamese cat. *Veterinary & Comparative Ophthalmology*, **4**, 121–124.

Brown, A.S., Leamen, L., Cucevic, V., et al. (2005) Quantitation of hemodynamic function during developmental vascular regression in the mouse eye. *Investigative Ophthalmology & Visual Science*, **46**, 2231–2237.

Brown, E.A., Thomasy, S.M., Murphy, C.J., & Bannasch, D.L. (2018) Genetic analysis of optic nerve head coloboma in the Nova Scotia Duck Tolling Retriever identifies discordance with the NHEJ1 intronic deletion (Collie eye anomaly mutation). *Veterinary Ophthalmology*, **21**, 144–150.

Brown, T., Delahunta, A., Bistner, S., et al. (1975) Pathogenetic studies of infection of the bovine fetus with bovine viral diarrhea virus: II. Ocular lesions. *Veterinary Pathology*, **12**, 394–404.

Browning, J., Reichelt, M.E., Gole, G.A., et al. (2001) Proximal arterial vasoconstriction precedes regression of the hyaloid vasculature. *Current Eye Research*, **22**, 405–411.

Bryden, M.M., Evans, H.E., & Keeler, R.F. (1971) Cyclopia in sheep caused by plant teratogens. *Journal of Anatomy*, **110**, 507–510.

Bumsted, K.M. & Barnstable, C.J. (2000) Dorsal retinal pigment epithelium differentiates as neural retina in the microphthalmia (mi/mi) mouse. *Investigative Ophthalmology & Visual Science*, **41**, 903–908.

Buyukmihci, N.C., Murphy, C.J., & Schulz, T. (1988) Developmental ocular disease of raptors. *Journal of Wildlife Diseases*, **24**, 207–213.

Carrig, C.B., Sponenberg, D.P., Schmidt, G.M., et al. (1988) Inheritance of associated ocular and skeletal dysplasia in Labrador Retrievers. *Journal of the American Veterinary Medical Association*, **193**, 1269–1272.

Cohen, A.I. (1961) Electron microscopic observations of the developing mouse eye: I. Basement membranes during early development and lens formation. *Developmental Biology*, **3**, 297–316.

Cohen, M.M. & Sulik, K.K.(1992) Perspectives on holoprosencephaly: Part II. Central nervous system, craniofacial anatomy, syndrome commentary, diagnostic approach, and experimental studies. *Journal of Craniofacial Genetics and Developmental Biology*, **12**, 196–244.

Collins, B.K., Collier, L.L., Johnson, G.S., et al. (1992) Familial cataracts and concurrent ocular anomalies in Chow Chows. *Journal of the American Veterinary Medical Association*, **200**, 1485–1491.

Cook, C. (1989) Experimental models of anterior segment dysgenesis. *Ophthalmic Paediatrics and Genetics*, **10**, 33–46.

Cook, C. (1995) Embryogenesis of congenital eye malformations. *Veterinary & Comparative Ophthalmology*, **5**, 109–123.

Cook, C., Burling, K., & Nelson, E. (1991a) Embryogenesis of posterior segment colobomas in the Australian Shepherd dog. *Progress in Veterinary & Comparative Ophthalmology*, **1**, 163–170.

Cook, C. & Sulik, K. (1986) Sequential scanning electron microscopic analyses of normal and spontaneously abnormal ocular development in C57b1/6j mice. *Scanning Electron Microscopy*, **3**, 1215–1227.

Cook, C. & Sulik, K. (1988) Keratolenticular dysgenesis (Peters' anomaly) as a result of acute embryonic insult during gastrulation. *Journal of Pediatric Ophthalmology and Strabismus*, **25**, 60–66.

Cook, C.S., Generoso, W.M., Hester, D., et al. (1991b) RPE dysplasia with retinal duplication in a mutant mouse strain. *Experimental Eye Research*, **52**, 409–415.

Cook, C.S., Nowotny, A.Z., & Sulik, K.K. (1987) Fetal alcohol syndrome: Eye malformations in a mouse model. *Archives of Ophthalmology*, **105**, 1576–1581.

Cook, C.S. & Sulik, K.K. (1990) Laminin and fibronectin in retinoid induced keratolenticular dysgenesis. *Investigative Ophthalmology & Visual Science*, **31**, 751–757.

Cooper, M.K., Porter, J.A., Young, K.E., et al. (1998) Teratogen mediated inhibition of target tissue response to shh signaling. *Science*, **280**, 1603–1607.

Coulombre, A. (1956) The role of intraocular pressure in the development of the chick eye. *Journal of Experimental Zoology*, **133**, 211–225.

Coulombre, A.J. & Coulombre, J.L. (1964) Lens development: I. Role of the lens in eye growth. *Journal of Experimental Zoology*, **156**, 39–47.

Coulombre, J. & Coulombre, A. (1969) Lens development: IV. Size, shape and orientation. *Investigative Ophthalmology & Visual Science*, **8**, 251–257.

Engelhardt, M., Wachs, F.P., Couillard-Despres, S., et al. (2004) The neurogenic competence of progenitors from the postnatal rat retina *in vitro*. *Experimental Eye Research*, **78**, 1025–1036.

Erlich, R.B., Werneck, C.C., Mourao, P.A.S., et al. (2003) Major glycosaminoglycan species in the developing retina: Synthesis, tissue distribution and effects upon cell death. *Experimental Eye Research*, **77**, 157–165.

Ewart, S.L., Ramsey, D.T., Xu, J., et al. (2000) The horse homolog of congenital aniridia conforms to codominant inheritance. *Journal of Heredity*, **91**, 93–98.

Feeney, S.A., Simpson, D.A.C., Gardiner, T.A., et al. (2003) Role of vascular endothelial growth factor and placental growth factors during retinal vascular development and hyaloid regression. *Investigative Ophthalmology & Visual Science*, **44**, 839–847.

Fischer, A.J. (2005) Neural regeneration in the chick retina. *Progress in Retinal and Eye Research*, **24**, 161–182.

Fitch, J., Fini, M.E., Beebe, D.C., et al. (1998) Collagen type IX and developmentally regulated swelling of the avian primary corneal stroma. *Developmental Dynamics*, **212**, 27–37.

Flower, R.W., McLeod, D.S., Lutty, G.A., et al. (1985) Postnatal retinal vascular development of the puppy. *Investigative Ophthalmology & Visual Science*, **26**, 957–968.

Fox, M. (1963) Postnatal ontogeny of the canine eye. *Journal of the American Veterinary Medical Association*, **143**, 968–974.

Fruttiger, M. (2002) Development of the mouse retinal vasculature: Angiogenesis versus vasculogenesis. *Investigative Ophthalmology & Visual Science*, **43**, 522–527.

Garcia-Porrero, J., Collado, J. & Ojeda, J. (1979) Cell death during detachment of the lens rudiment from ectoderm in the chick embryo. *Anatomical Record*, **193**, 791–804.

Gelatt, K., Huston, K., & Leipold, H. (1969) Ocular anomalies of incomplete albino cattle: Ophthalmoscopic examination. *American Journal of Veterinary Research*, **30**, 1313–1316.

Gelatt, K., Samuelson, D., Barrie, K., et al. (1983) Biometry and clinical characteristics of congenital cataracts and microphthalmia in the Miniature Schnauzer. *Journal of the American Veterinary Medical Association*, **183**, 99–102.

Gelatt, K.N. & McGill, L.D. (1973). Clinical characteristics of microphthalmia with colobomas of the Australian Shepherd Dog. *Journal of the American Veterinary Medical Association*, **162**, 393–396.

Gelatt, K.N. & Veith, L.A. (1970) Hereditary multiple ocular anomalies in Australian shepherd dogs. (preliminary report). *Veterinary Medicine, Small Animal Clinician*, **65**, 39–42.

Gemensky-Metzler, A.J., Wilkie, D.A., & Cook, C.S. (2004) The use of semiconductor diode laser for deflation and coagulation of anterior uveal cysts in dogs, cats and horses: A report of 20 cases. *Veterinary Ophthalmology*, **7**, 360–368.

Glaze, M.B. (2005) Congenital and hereditary ocular abnormalities in cats. *Clinical Techniques in Small Animal Practice*, **20**, 74–82.

Grainger, R., Henry, J., & Henderson, R. (1988) Reinvestigation of the role of the optic vesicle in embryonic lens induction. *Development*, **102**, 517–526.

Grainger, R.M., Henry, J.J., Saha, M.S., et al. (1992) Recent progress on the mechanisms of embryonic lens formation. *Eye*, **6**, 117–122.

Greene, H. & Leipold, H. (1974) Hereditary internal hydrocephalus and retinal dysplasia in Shorthorn calves. *Cornell Veterinarian*, **64**, 367–375.

Greiner, J.V. & Weidman, T.A. (1980) Histogenesis of the cat retina. *Experimental Eye Research*, **30**, 439–453.

Greiner, J.V. & Weidman, T.A. (1981) Histogenesis of the ferret retina. *Experimental Eye Research*, **33**, 315–332.

Greiner, J.V. & Weidman, T.A. (1982) Embryogenesis of the rabbit retina. *Experimental Eye Research*, **34**, 749–765.

Gwin, R., Wyman, M., Lim, D., et al. (1981) Multiple ocular defects associated with partial albinism and deafness. *Journal of the American Animal Hospital Association*, **17**, 401.

Hale, F. (1935) The relation of vitamin A to anophthalmos in pigs. *American Journal of Ophthalmology*, **18**, 1087–1093.

Hamoudi, H., Rudnick, J.-C., Prause, J.U., et al. (2013) Anterior segment dysgenesis (Peters' anomaly) in two snow leopard (Panthera uncia) cubs. *Veterinary Ophthalmology*, **16**, 130–134.

Hartwig, N.G., Vermeij-Keers, C., & Versteeg, J. (1988) The anterior eye segment in virus-induced primary congenital aphakia. *Acta Morphologica Neerlando-Scandinavica*, **26**, 283–292.

Hay, E. (1980) Development of the vertebrate cornea. *International Review of Cytology*, **63**, 263–322.

Hay, E. & Revel, J. (1969) Fine structure of the developing avian cornea. In: *Monographs in Developmental Biology* (eds Wolsky, A. & Chen, P.S.), Vol. **1**, pp. 1–144. Basel: Karger.

Hero, I., Farjah, M., & Scholtz, C.L. (1991) The prenatal development of the optic fissure in colobomatous microphthalmia. *Investigative Ophthalmology & Visual Science*, **32**, 2622–2635.

Heywood, R. & Wells, G. (1970) A retinal dysplasia in the Beagle dog. *Veterinary Record*, **87**, 178–180.

Hilfer, S. (1983) Development of the eye of the chick embryo. *Scanning Electron Microscopy*, **III**, 1353–1369.

Hilfer, S., Brady, R., & Yank, J. (1981) Intracellular and extracellular changes during early ocular development in the chick embryo. In: *Ocular Size and Shape: Regulation during Development* (eds Hilfer, S. & Sheffield, J.), pp. 47–78. New York: Springer-Verlag.

Hilfer, S.R. & Randolph, G.J. (1993) Immunolocalization of basal lamina components during development of chick otic and optic primordia. *Anatomical Record*, **235**, 443–452.

Holle, D.M., Stankovics, M.E., Sarna, C.S., et al. (1999) The geographic form of retinal dysplasia in dogs is not always a congenital abnormality. *Veterinary Ophthalmology*, **2**, 61–66.

Horrigan, S.K., Rich, C.B., Streeten, B.W., et al. (1992) Characterization of an associated microfibril protein through recombinant DNA techniques. *Journal of Biological Chemistry*, **267**, 10087–10095.

Hubmacher, D., Reinhardt, D.P., Plesec, T., et al. (2014) Human eye development is characterized by coordinated expression of fibrillin isoforms. *Investigative Ophthalmology & Visual Science*, **55**, 7934–7944.

Hughes, S., Yang, H.J., & Chan-Ling, T. (2000) Vascularization of the human fetal retina: Roles of vasculogenesis and angiogenesis. *Investigative Ophthalmology & Visual Science*, **41**, 1217–1228.

Hunt, H.H. (1961) A study of the fine structure of the optic vesicle and lens placode of the chick embryo during incubation. *Developmental Biology*, **3**, 175–209.

Ikeda, K., Shirai, S., Majima, A., et al. (1995) Histological and histochemical studies of normal and faulty closure of the embryonic fissure in the eye of ICR mouse. *Japanese Journal of Ophthalmology*, **39**, 20–29.

Incardona, J.P., Gaffield, W., Kapur, R.P., et al. (1998) The teratogenic veratrum alkaloid cyclopamine inhibits sonic hedgehog signal transduction. *Development*, **125**, 3553–3562.

Incardona, J.P., Gaffield, W., Lange, Y., et al. (2000) Cyclopamine inhibition of Sonic hedgehog signal transduction is not mediated through effects on cholesterol transport. *Developmental Biology*, **224**, 440–452.

Irby, N.L. & Aguirre, G.D. (1985) Congenital aniridia in a pony. *Journal of the American Veterinary Medical Association*, **186**, 281–283.

Ito, M. & Yoshioka, M. (1999) Regression of the hyaloid vessels and pupillary membrane of the mouse. *Anatomy and Embryology*, **200**, 403–411.

Jack, R. (1972) Regression of the hyaloid vascular system: An ultrastructural analysis. *American Journal of Ophthalmology*, **74**, 261–272.

Jacobson, A.G. (1988) Somitomeres: Mesodermal segments of vertebrate embryos. *Development*, **104** (Suppl.), 209–220.

Johns, P.R., Rusoff, A.C., & Dubin, M.W. (1979) Postnatal neurogenesis in the kitten retina. *Journal of Comparative Neurology*, **187**, 545–555.

Johnston, M.C., Noden, D.M., Hazelton, R.D., et al. (1979) Origins of avian ocular and periocular tissues. *Experimental Eye Research*, **29**, 27–43.

Jones, K., Higginbottom, M. & Smith, D. (1980) Determining the role of the optic vesicle in orbital and periocular development and placement. *Pediatric Research*, **14**, 703–708.

Kahrs, R., Scott, F., & De Lahunta, A. (1970) Congenital cerebellar hypoplasia and ocular defects in calves following bovine virus diarrhea-mucosal disease infection in pregnant cattle. *Journal of the American Veterinary Medical Association*, **156**, 1443.

Kaswan, R.L., Collins, L.G., Blue, J.L., et al. (1987) Multiple hereditary ocular anomalies in a herd of cattle. *Journal of the American Veterinary Medical Association*, **191**, 97–99.

Keeler, R.F. (1990) Teratogenic compounds of *Veratrum californicum* (durand): X. Cyclopia in rabbits produced by cyclopamine. *Teratology*, **3**, 175–180.

Keeler, R.F. & Binns, W. (1966) Teratogenic compounds of *Veratrum californicum* (durand): II. Production of ovine fetal cyclopia by fractions and alkaloid preparations. *Canadian Journal of Biochemistry*, **44**, 829–838.

Kern, T.J. (1981) Persistent hyperplastic primary vitreous and microphthalmia in a dog. *Journal of the American Veterinary Medical Association*, **178**, 1169–1171.

Koch, S.A. (1979) Congenital ophthalmic abnormalities in the Burmese cat. *Journal of American Veterinary Medical Association*, **174**, 90–91.

Komaromy, A.M., Rowlan, J.S., La Croix, N.C., et al. (2011) Equine multiple congenital ocular anomalies (MCOA) syndrome in PMEL17 (Silver) mutant ponies: Five cases. *Veterinary Ophthalmology*, **14**, 313–320.

Kupfer, C. & Kaiser-Kupfer, M.I. (1978) New hypothesis of developmental anomalies of the anterior chamber associated with glaucoma. *Transactions of the Ophthalmology Society of the United Kingdom*, **98**, 213–215.

Kupfer, C. Kuwabara, T., & Stark, W.J. (1975) The histopathology of Peters' anomaly. *American Journal of Ophthalmology*, **80**, 653–660.

Laratta, L.J., Riis, R.C., Kern, T.J., et al. (1985) Multiple congenital ocular defects in the Akita dog. *Cornell Veterinarian*, **75**, 381–392.

Lavach, D.D., Murphy, J.M., & Severin, G.A. (1978) Retinal dysplasia in the English Springer Spaniel. *Journal of the American Animal Hospital Association*, **14**, 192–199.

LeDouarin, N. & Teillet, M. (1974) Experimental analysis of the migration and differentiation of neuroblasts of the autonomic nervous system and of neurectodermal mesenchymal derivatives, using a biological cell marking technique. *Developmental Biology*, **41**, 162–184.

Lewis, D., Kelly, D., & Sansom, J. (1986) Congenital microphthalmia and other developmental ocular anomalies in the Dobermann. *Journal of Small Animal Practice*, **27**, 559–566.

Los, L.I., van Luyn, M.J.A., Eggli, P.S., et al. (2000a) Vascular remnants in the rabbit vitreous body: II. Enzyme digestion and immunohistochemical studies. *Experimental Eye Research*, **71**, 153–165.

Los, L.I., van Luyn, M.J.A., & Nieuwenhuis, P. (2000b) Vascular remnants in the rabbit vitreous body: I. Morphological characteristics and relationship to vitreous embryonic development. *Experimental Eye Research*, **71**, 143–151.

Lowe, J.K., Kukekova, A.V., Kirkness, E.F., et al. (2003) Linkage mapping of the primary disease locus for Collie eye anomaly. *Genomics*, **82**, 86–95.

MacMillan, A. & Lipton, D. (1978) Heritability of multifocal retinal dysplasia in American Cocker Spaniels. *Journal of the American Veterinary Medical Association*, **172**, 568–572.

Maestro De Las Casas, C., Epeldegui, M., Tudela, C., et al. (2003) High exogenous homocysteine modifies eye development in early chick embryos. *Birth Defects Research. Part A, Clinical and Molecular Teratology*, **67**, 35–40.

Manoly, R. (1951) Blindness in newborn pigs. *Veterinary Record*, **63**, 398.

Martin, A.C., Thornton, J.D., Liu, J., et al. (2004) Pathogenesis of persistent hyperplastic primary vitreous in mice lacking the Arf tumor suppressor gene. *Investigative Ophthalmology & Visual Science*, **45**, 3387–3396.

Martin, C. (1974) Development of the pectinate ligament structure of the dog. *American Journal of Veterinary Research*, **35**, 1433.

Martin, C. (1978) Strabismus associated with extraocular muscle agenesis in a dog. *Journal of the American Animal Hospital Association*, **14**, 486–489.

Martin, C. & Wyman, M. (1968) Glaucoma in the Basset Hound. *Journal of the American Veterinary Medical Association*, **153**, 1320–1327.

Martin, C.L. & Leipold, H.W. (1974) Aphakia and multiple ocular defects in Saint Bernard puppies. *Veterinary Medicine, Small Animal Clinician*, **69**, 448–453.

Martin, C.L., Stiles, J., & Willis, M. (1997) Feline colobomatous syndrome. *Veterinary & Comparative Ophthalmology*, **7**, 39–43.

Matsuura, T., Tsuji, N., Kodama, Y., et al. (2013) Iridal coloboma induces dyscoria during miosis in FLS mice. *Veterinary Ophthalmology*, **16**, 186–191.

Meier, S. (1982) The development of segmentation in the cranial region of vertebrate embryos. *Scanning Electron Microscopy,* **Pt 3**, 1269–1282.

Meier, S. & Tam, P.P. (1982) Metameric pattern development in the embryonic axis of the mouse: I. *Differentiation of the cranial segments. Differentiation*, **21**, 95–108.

Meyers, V.N., Jezyk, P.F., Aguirre, G.D., et al. (1983) Short-limbed dwarfism and ocular defects in the Samoyed dog. *Journal of the American Veterinary Medical Association*, **183**, 975–979.

Miller, M.T., Epstein, R.J., Sugar, J., et al. (1984) Anterior segment anomalies associated with the fetal alcohol syndrome. *Journal of Pediatric Ophthalmology and Strabismus*, **21**, 8–18.

Molleda, J.M., Martin, E., Ginel, P.J., et al. (1995) Microphakia associated with lens luxation in the cat. *Journal of the American Animal Hospital Association*, **31**, 209–212.

Monaco, M., Samuelson, D., & Gelatt, K. (1985) Morphology and postnatal development of the normal lens in the dog and congenital cataract in the Miniature Schnauzer. *Lens Research*, **2**, 393–433.

Montiani-Ferreira, F., Petersen-Jones, S., Cassotis, N., et al. (2003) Early postnatal development of central corneal thickness in dogs. *Veterinary Ophthalmology*, **6**, 19–22.

Moore, C.P., Shaner, J.B., Halenda, R.M., et al. (1999) Congenital ocular anomalies and ventricular septal defect in a Dromedary camel (*Camelus dromedarius*). *Journal of Zoo and Wildlife Medicine*, **30**, 423–430.

Mulder, G.B., Manley, N., Grant, J., et al. (2000) Effects of excess vitamin A on development of cranial neural crest-derived structures: A neonatal and embryologic study. *Teratology*, **62**, 214–226.

Munyard, K.A., Sherry, C.R., & Sherry, L. (2007) A retrospective evaluation of congenital ocular defects in Australian Shepherd dogs in Australia. *Veterinary Ophthalmology*, **10**, 19–22.

Murphy, C.J., Kern, T.J., Loew, E., et al. (1985) Retinal dysplasia in a hybrid falcon. *Journal of the American Veterinary Medical Association*, **187**, 1208–1209.

Mutlu, F. & Leipold, I. (1964) The structure of the fetal hyaloid system and tunica vasculosa lentis. *Archives of Ophthalmology*, **71**, 102–110.

Nakano, K.E. & Nakamura, H. (1985) Origin of the irideal striated muscle in birds. *Journal of Embryology and Experimental Morphology*, **88**, 1–13.

Narfstrom, K. (1999) Hereditary and congenital ocular disease in the cat. *Journal of Feline Medicine Surgery*, **1**, 135–141.

Narfstrom, K. & Dubielzig, R. (1984) Posterior lenticonus, cataracts and microphthalmia in the Cavalier King Charles Spaniel. *Journal of Small Animal Practice*, **25**, 669–677.

Nelson, D. & Macmillan, A. (1983) Multifocal retinal dysplasia in field trial Labrador Retrievers. *Journal of the American Animal Hospital Association*, **19**, 388–392.

Njoku, C.O., Esievo, K.A., Bida, S.A., et al. (1978) Canine cyclopia. *Veterinary Record*, **102**, 60–61.

Noden, D. (1993) Periocular mesenchyme: Neural crest and mesodermal interactions. In: *Duane's Foundations of Clinical Ophthalmology* (eds Tasman, W. & Jaeger, E.), pp. 1–23. Hagerstown, MD: Lippincott.

Noden, D.M. (1986) Patterning of avian craniofacial muscles. *Developmental Biology*, **116**, 347–356.

O'Rahilly, R. (1983) The timing and sequence of events in the development of the human eye and ear during the embryonic period proper. *Anatomy and Embryology*, **168**, 87–99.

Ori, J.I., Yoshikai, T., Yoshimur, S., et al. (2000) Posterior lenticonus with congenital cataract in a Shih Tzu dog. *Journal of Veterinary Medical Science*, **62**, 1201–1203.

O'Toole, D., Young, S., Severin, G.A., et al. (1983) Retinal dysplasia of English Springer Spaniel dogs: Light microscopy of the postnatal lesions. *Veterinary Pathology*, **20**, 298–311.

Ozeki, H., Ogura, Y., Hirabayashi, Y., et al. (2000) Apoptosis is associated with formation and persistence of the embryonic fissure. *Current Eye Research*, **20**, 367–372.

Ozeki, H., Ogura, Y., Hirabayashi, Y., et al. (2001) Suppression of lens stalk cell apoptosis by hyaluronic acid leads to faulty separation of the lens vesicle. *Experimental Eye Research*, **72**, 63–70.

Packard, D.S. & Meier, S. (1983) An experimental study of the somitomeric organization of the avian segmental plate. *Developmental Biology*, **97**, 191–202.

Pearl, R., Gould, D., & Spiess, B. (2015) Progression of pectinate ligament dysplasia over time in two populations of Flat-Coated Retrievers. *Veterinary Ophthalmology*, **18**, 6–12.

Peiffer, R. (1982) Bilateral congenital aphakia and retinal detachment in a cat. *Journal of the American Animal Hospital Association*, **18**, 128–130.

Peiffer, R. & Fischer, C. (1983) Microphthalmia, retinal dysplasia and anterior segment dysgenesis in a litter of Doberman Pinschers. *Journal of the American Veterinary Medical Association*, **183**, 875.

Percy, D., Scott, F., & Albert, D. (1975) Retinal dysplasia due to feline panleukopenia virus infection. *Journal of the American Veterinary Medical Association*, **167**, 935–937.

Perveen, R., Lloyd, I.C., Clayton-Smith, J., et al. (2000) Phenotypic variability and asymmetry of Rieger syndrome associated with PITX2 mutations. *Investigative Ophthalmology & Visual Science*, **41**, 2456–2460.

Pinard, C.L. & Basrur, P.K. (2011) Ocular anomalies in a herd of Exmoor ponies in Canada. *Veterinary Ophthalmology*, **14**, 100–108.

Plummer, C.E. & Ramsey, D.T. (2011) A survey of ocular abnormalities in miniature horses. *Veterinary Ophthalmology*, **14**, 239–243.

Pumphrey, S.A., Pizzirani, S., Pirie, C.G., & Needle, D.B. (2013) Glaucoma associated with uveal cysts and goniodysgenesis in American Bulldogs: A case series. *Veterinary Ophthalmology*, **16**, 377–385.

Ramsey, D.T., Ewart, S.L., Render, J.A., et al. (1999a) Congenital ocular abnormalities of Rocky Mountain horses. *Veterinary Ophthalmology*, **2**, 47–59.

Ramsey, D.T., Hauptman, J.G., & Petersen-Jones, S.M. (1999b) Corneal thickness, intraocular pressure, and optical corneal diameter in Rocky Mountain horses with cornea globosa or clinically normal corneas. *American Journal of Veterinary Research*, **60**, 1317–1321.

Rebhun, R. (1977) Congenital anterior staphyloma with rudimentary lens in a calf. *Journal of the American Veterinary Medical Association*, **171**, 440–442.

Reme, C., Urner, U., & Aeberhard, B. (1983a) The development of the chamber angle in the rat eye. *Graefe's Archive for Clinical and Experimental Ophthalmology*, **220**, 139–153.

Reme, C., Urner, U., & Aeberhard, B. (1983b) The occurrence of cell death during the remodelling of the chamber angle recess in the developing rat eye. *Graefe's Archive for Clinical and Experimental Ophthalmology*, **221**, 113–121.

Roberts, L. (1948) Microphthalmia in swine. *Journal of Heredity*, **39**, 146.

Roberts, S.R. & Bistner, S.I. (1968) Persistent pupillary membrane in Basenji dogs. *Journal of the American Veterinary Medical Association*, **153**, 533–542.

Rodarte-Almeida, A.C.V., Petersen-Jones, S., Langohr, I.M., et al. (2016) Retinal dysplasia in American Pit Bull terriers – phenotypic characterization and breeding study. *Veterinary Ophthalmology*, **19**, 11–21.

Rubin, L. (1963) Hereditary retinal detachment in Bedlington Terriers: A preliminary report. *Veterinary Medicine, Small Animal Clinician*, **3**, 387–389.

Rubin, L. (1968) Heredity of retinal dysplasia in Bedlington Terriers. *Journal of the American Veterinary Medical Association*, **152**, 260–262.

Rubin, L., Nelson, E., & Sharp, C. (1991) Collie eye anomaly in Australian Shepherd dogs. *Progress in Veterinary & Comparative Ophthalmology*, **1**, 105–108.

Rupp, G. & Knight, A. (1984) Congenital ocular defects in a crossbred beef herd. *Journal of the American Veterinary Medical Association*, **184**, 1149–1150.

Samuelson, D. & Gelatt, K. (1984a) Aqueous outflow in the Beagle: Postnatal development of the pectinate ligament and trabecular meshwork. *Current Eye Research*, **3**, 783.

Samuelson, D. & Gelatt, K. (1984b) Aqueous outflow in the Beagle: II. Postnatal morphologic development of the iridocorneal angle: Corneoscleral trabecular meshwork and angular aqueous plexus. *Current Eye Research*, **3**, 795–807.

Samuelson, D., Das, N., Bauer, J., et al. (1987) Prenatal morphogenesis of the congenital cataracts in the Miniature Schnauzer. *Lens Research*, **180**, 231–250.

Saperstein, G. (1975) Congenital defects in sheep. *Journal of the American Veterinary Medical Association*, **167**, 314.

Saunders, L. & Fincher, M. (1951) Hereditary multiple eye defects in grade Jersey calves. *Cornell Veterinarian*, **41**, 351–366.

Schaepdrijver, L.D., Simoens, P., Lauwers, H., et al. (1989) The hyaloid vascular system of the pig. *Anatomy and Embryology*, **1989**, 549–554.

Schiavo, D.M. & Field, W.E. (1974) Unilateral focal retinal dysplasia in Beagle dogs. *Veterinary Medicine, Small Animal Clinician*, **69**, 33–34.

Schook, P. (1978) A review of data on cell actions and cell interactions during the morphogenesis of the embryonic eye. *Acta Morphologica Neerlando-Scandinavica*, **16**, 267–286.

Sevel, D. (1981) Reappraisal of the origin of human extraocular muscles. *Ophthalmology*, **88**, 1330.

Sevel, D. (1986) The origins and insertions of the extraocular muscles: Development, histologic features, and clinical significance. *Transactions of the American Ophthalmological Society*, **84**, 488–526.

Shields, M., Buckley, E., Klintworth, G., et al. (1985) Axenfeld–Rieger syndrome. A spectrum of developmental disorders. *Survey of Ophthalmology*, **29**, 387–409.

Shively, J., Phemister, R., Epling, G., et al. (1970) Pathogenesis of radiation-induced retinal dysplasia. *Investigative Ophthalmology & Visual Science*, **9**, 888–900.

Shively, J., Phemister, R., Epling, G., et al. (1972) Dose relationships of pathologic alterations in the developing retina of irradiated dogs. *American Journal of Veterinary Research*, **33**, 2121–2134.

Shively, J.N., Epling, G.P., & Jensen, R. (1971) Fine structure of the postnatal development of the canine retina. *American Journal of Veterinary Research*, **32**, 383–392.

Silverstein, A. & Al, E. (1971) An experimental virus-induced retinal dysplasia in the fetal lamb. *American Journal of Ophthalmology*, **72**, 22.

Smelser, G. & Ozanics, V. (1971) The development of the trabecular meshwork in primate eyes. *American Journal of Ophthalmology*, **71**, 366.

Sonoda, S., Isashiki, Y., Tabata, Y., et al. (2000) A novel PAX6 gene mutation (P118R) in a family with congenital nystagmus associated with a variant form of aniridia. *Graefe's Archive for Clinical and Experimental Ophthalmology*, **238**, 552–558.

Spira, A.W. & Hollenberg, M.J. (1973) Human retinal development: Ultrastructure of the inner retinal layers. *Development Biology*, **31**, 1–21.

Stades, F. (1980) Persistent hyperplastic tunica vasculosa lentis and persistent hyperplastic primary vitreous (PHTVL/PHPV) in 90 closely related Doberman Pinschers: Clinical aspects. *Journal of the American Animal Hospital Association*, **16**, 739–751.

Stades, F. (1983) Persistent hyperplastic tunica vasculosa lentis and persistent hyperplastic primary vitreous in Doberman Pinschers: Genetic aspects. *Journal of the American Animal Hospital Association*, **19**, 957–964.

Strande, A., Nicolaissen, B., & Bjerkas, I. (1988) Persistent pupillary membrane and congenital cataract in a litter of English Cocker Spaniels. *Journal of Small Animal Practice*, **29**, 257–260.

Stromland, K., Miller, M., & Cook, C. (1991) Ocular teratology. *Survey of Ophthalmology*, **35**, 429–446.

Sulik, K.K. & Johnston, M.C. (1982) Embryonic origin of holoprosencephaly: Interrelationship of the developing brain and face. *Scanning Electron Microscopy*, **Pt 1**, 309–322.

Swanson, H.L., Dubielzig, R.R., Bentley, E., et al. (2001) A case of Peters' anomaly in a Springer Spaniel. *Journal of Comparative Pathology*, **125**, 326–330.

Tam, P.P. (1986) A study of the pattern of prospective somites in the presomitic mesoderm of mouse embryos. *Journal of Embryology and Experimental Morphology*, **92**, 269–285.

Tam, P.P. & Trainor, P.A.A. (1994) Specification and segmentation of the paraxial mesoderm. *Anatomy and Embryology (Berlin)*, **189**, 275–305.

Tam, P.P., Meier, S., & Jacobson, A.G. (1982) Differentiation of the metameric pattern in the embryonic axis of the mouse: II. Somitomeric organization of the presomitic mesoderm. *Differentiation*, **21**, 109–122.

Townsend, W. M. & Gornik, K.R. (2013) Prevalence of uveal cysts and pigmentary uveitis in Golden Retrievers in three Midwestern states. *Journal of the American Veterinary Medical Association*, **243**, 1298–1301.

Trainor, P.A. & Tam, P.P. (1995) Cranial paraxial mesoderm and neural crest cells of the mouse embryo: Co-distribution in the craniofacial mesenchyme but distinct segregation in branchial arches. *Development*, **121**, 2569–2582.

van der Linde-Sipman, J., Stades, F., & De Wolff-Rouendaal, D. (1983) Persistent hyperplastic tunica vasculosa lentis and persistent hyperplastic primary vitreous in the Doberman Pinscher: Pathological aspects. *Journal of the American Animal Hospital Association*, **19**, 791–802.

van der Linde-Sipman, J.S., van den Ingh, T.S.G.A.M., & Vellema, P. (2003) Morphology and morphogenesis of hereditary microphthalmia in Texel sheep. *Journal of Comparative Pathology*, **128**, 269–275.

van Rensburg, I.B.J., Petrick, S.W., van der Lugt, J., et al. (1992) Multiple inherited eye anomalies including persistent hyperplastic tunica vasculosa lentis in Bouvier des Flandres. *Veterinary & Comparative Ophthalmology*, **2**, 133–139.

Wahl, C.M., Noden, D.M., & Baker, R. (1994) Developmental relations between sixth nerve motor neurons and their targets in the chick embryo. *Developmental Dynamics*, **201**, 191–202.

Waring, G., Rodriques, M., & Laibson, P. (1975) Anterior chamber cleavage syndrome: A stepladder classification. *Survey of Ophthalmology*, **20**, 3–33.

Weiss, P. & Jackson, S.F. (1961) Fine structural changes associated with lens determination in the avian embryo. *Developmental Biology*, **3**, 532–554.

Whiteley, H. (1991) Dysplastic canine retinal morphogenesis. *Investigative Ophthalmology & Visual Science*, **32**, 1492–1498.

Wrenn, J. & Wessells, N. (1969) An ultrastructural study of lens invagination in the mouse. *Journal of Experimental Zoology*, **171**, 359–368.

Wulle, K. (1972) The development of the productive and draining system of the aqueous humor in the eye. *Advances in Ophthalmology*, **26**, 296–355.

Wyand, D., Lehav, M., Albert, D., et al. (1972) Intraocular lacrimal gland tissue with other ocular abnormalities occurring in a white-tailed deer. *Journal of Comparative Pathology*, **82**, 219–221.

Wyman, M. & Ketring, K. (1976) Congenital glaucoma in the Basset Hound: A biologic model. *Transactions. Section on Ophthalmology. American Academy of Ophthalmology and Otolaryngology*, **81**, OP645–OP652.

Yamashita, T. & Sohal, G. (1986) Development of smooth and skeletal muscle cells in the iris of the domestic duck, chick and quail. *Cell and Tissue Research*, **244**, 121–131.

Yamashita, T. & Sohal, G. (1987) Embryonic origin of skeletal muscle cells in the iris of the duck and quail. *Cell and Tissue Research*, **249**, 31–37.

Zhang, R.L., Samuelson, D.A., Zhang, Z.G., et al. (1991) Analysis of eye lens-specific genes in congenital hereditary cataracts and microphthalmia of the Miniature Schnauzer dog. *Investigative Ophthalmology & Visual Science*, **32**, 2662–2665.

Zhao, S. & Overbeek, P.A. (2001) Regulation of choroid development by the retinal pigment epithelium. *Molecular Vision*, **7**, 277–282.

Zhu, M.D., Madigan, M.C., van Driel, D., et al. (2000) The human hyaloid system: Cell death and vascular regression. *Experimental Eye Research*, **70**, 767–776.